



ELSEVIER

Catalysis Today 50 (1999) 175–206



Some recent results on metal/support interaction effects in NM/CeO₂ (NM: noble metal) catalysts

S. Bernal^{*}, J.J. Calvino, M.A. Cauqui, J.M. Gatica, C. Larese, J.A. Pérez Omil, J.M. Pintado

*Departamento de Ciencia de los Materiales, Ingeniería Metalúrgica y Química Inorgánica, Facultad de Ciencias, Universidad de Cádiz,
Apartado 40, Puerto Real, 11510, Cádiz, Spain*

Abstract

In this work, some recent chemical and nanostructural characterisation studies on ceria-supported noble metal (NM/CeO₂; NM: Rh, Pd, Pt) catalysts are reviewed. According to the information available, a proposal is made about the nature of the metal/support interaction phenomena occurring in NM/CeO₂ catalysts as the reduction temperature is increased. By combining the information provided by the HREM and the hydrogen chemisorption (volumetric adsorption, TPD-MS and H₂/D₂ isotopic exchange) studies, it is proposed that, for reduction temperatures up to 773 K, the observed partial deactivation effects are mainly due to electronic metal/support interactions. Metal decoration phenomena do also occur on the three NM/CeO₂ catalysts. In contrast with that reported for NM/TiO₂, however, they have only been observed upon reduction at 873 (Pd) or 973 K (Rh, Pt). At the highest reduction temperature, 1173 K, a crystallographically well-defined alloy phase could only be observed on Pt/CeO₂ (CePt₅). On Pd/CeO₂ a solid solution of Ce in Pd may also be formed. The phases resulting from the reoxidation of the decorated and/or alloyed metal microcrystals have also been characterised by means of HREM. Significant differences with the NM/TiO₂ catalysts are observed. The classic reoxidation treatment at 773 K does not allow the segregation of the NM and CeO₂ phases, and therefore no complete recovery of the catalytic systems is achieved. © 1999 Elsevier Science B.V. All rights reserved.

Keywords: NM/CeO₂ catalysts; Metal/support interaction; Electronic effects; Metal decoration; Alloying; Reoxidation effects

1. Introduction

Since Tauster et al. [1] reported for the first time on the so-called SMSI (strong metal–support interaction) effect, a great deal of research effort has been devoted to the subject. From a phenomenological point of view, the SMSI effect is characterised by a number of features which can be summarised as follows [1–3]:

1. it is associated with reducible supports;
2. it is induced by “high temperature”, typically $T_{\text{redn}} \geq 723$ K, reduction treatments;
3. inherent to the onset of the SMSI state, the chemical properties of the dispersed metal phase are heavily disturbed: strong inhibition of its chemisorptive properties and significant changes in its catalytic behaviour occur;
4. it is reversible, i.e., upon high-temperature reoxidation ($T_{\text{reoxn}} \geq 723$ K) followed by a mild reduction treatment, the conventional behaviour of the supported metal phase may be recovered.

^{*}Corresponding author. Fax: +34-956-834924; e-mail: serafin.bernal@uca.es

In the case of M/TiO_2 catalysts, the most representative example of a system exhibiting the SMSI effect, the major factors contributing to the onset of the SMSI state seem to be well-established. High resolution electron microscopy (HREM) [4–7] has provided direct experimental evidence on the occurrence of metal decoration (geometric effect) in Rh/TiO_2 catalysts reduced at 773 K. More recently [8], the HREM technique has also been used to establish the amorphous nature of the reduced titania phase partly covering the metal crystallites. Likewise, this technique has also been used to investigate the effect induced on a Rh/TiO_2 catalyst under the SMSI state by a reoxidation treatment at 673 K and further reduction at 473 K [8]. Though some nanostructural differences were observed between the recovered catalyst and that directly reduced at 473 K, the HREM study reported in [8] clearly shows the reversibility of the metal decoration effect. Finally, the NMR study of the hydrogen chemisorption on Rh/TiO_2 has quite convincingly proved that both electronic and geometric effects play an important role in determining the metal deactivation associated with the onset of the SMSI effect [9–11]. In fact, the results reported in [9] suggest that this effect is rather progressive, the electronic perturbation of the metal crystallites being observed at lower reduction temperatures than the geometric one.

1.1. Earlier studies of the strong metal/support interaction in M/CeO_2 catalysts

In accordance with the reducible nature of ceria [12–15], M/CeO_2 catalysts were soon included among the likely systems exhibiting some sort of strong metal/support interaction effects. Both experimental [16–24] and theoretical [25] studies reported in the 1980s support such a proposal. In these earlier studies, however, contradictory interpretations of the observed phenomena were offered. Thus, Sánchez and Gazquez [25], on the basis of structural considerations, established significant differences between the metal/support interactions occurring in M/TiO_2 and M/CeO_2 catalysts. In [25], the acronym SMSI is reserved for metals supported on oxides with cassiterite-type (SnO_2) structure, like TiO_2 -rutile. The authors suggest that, for M/TiO_2 catalysts, because of the open nature of the support cationic sublattice, the “high-tempera-

ture” reduction would induce the creation of vacancies at the support followed by diffusion of the metal atoms into the bulk of the reduced oxide. As a consequence of this burial effect, the chemisorptive and catalytic properties of the metal would become strongly disturbed. Subsequent “high-temperature” ($T_{\text{reoxn}} > 700$ K) reoxidation would drive the metal atoms back to the surface, so that a further mild reduction treatment would recover the chemisorptive and catalytic properties of the catalyst. This proposal, however, does not seem to be supported by the HREM studies commented above [4–8]. For oxide supports with fluorite-type structure, like ceria, Sánchez and Gazquez [25] suggest that the structure of the cationic sublattice would present a high barrier to penetration of the bulk by the metal atoms. Accordingly, they suggest the occurrence of a “nesting” effect, consisting of the anchoring of the metal atoms/crystallites in the oxygen vacancies created at the surface of the support. In this way, they justify the good resistance against sintering of the metal phase, as well as the high chemisorption capability and catalytic activity of the M/CeO_2 systems. In accordance with this interpretation, no detrimental chemical effects would be associated with the strong interaction phenomena occurring in ceria-supported metal catalysts [25].

Several other alternative proposals were suggested in these earlier studies. Thus, Meriaudeau et al. [16] have investigated the chemical effects induced on Pt/TiO_2 and Pt/CeO_2 by two different reduction treatments: 473 and 773 K. According to these authors, the latter treatment induces chemical changes on both catalysts. However, drastic inhibition of the chemisorptive capabilities could only be observed on Pt/TiO_2 . They conclude that the nature of the metal/support interactions were different in each case. Though not proved, Pt–Ce alloying was proposed as the likely origin of the observed effects in Pt/CeO_2 . In [21], on the contrary, an IR spectroscopy study of the CO adsorption on Pt/CeO_2 leads the author to conclude that upon increasing the reduction temperature from 673 to 973 K there is a significant loss of the metal chemisorption capability. This capability could be partly recovered by further reoxidation at 673 K. These observations were interpreted as due to the onset of an SMSI state, upon reduction at 973 K. In [21] purely electronic effects were suggested to be the most likely origin of the phenomenon.

As reported in a recent comprehensive review of the catalytic properties of ceria [26], the research activities on ceria-supported metal catalysts has steeply increased in the 1990s. In particular, the close connection of these systems with the three-way catalysts (TWCs), nowadays used in the control of exhaust emissions from motor vehicles [26,27], has very much stimulated the investigation on NM/CeO₂ (NM: Pt, Pd, Rh). Consequently, a good deal of information is at present available on Pt/CeO₂ [6,28–54], Pd/CeO₂ [23,28,30,33,41,51,55–76], and Rh/CeO₂ [7,28,30,33,38,41,44,46,50,51,77–126], and to a lesser extent on Ru/CeO₂ [30,71,127–129], Ir/CeO₂ [30,130–132], and Au/CeO₂ [133–135] systems. Likewise, studies on Ni/CeO₂ [40,136–146], Co/CeO₂ [129,147], and several other ceria-supported non-noble transition metal catalysts [40,133,134,139,148,149] have also been published.

In spite of the wealth of information available at present, there are still many uncertainties about the precise nature of the metal/support interaction phenomena occurring in ceria-supported metal catalysts [26]. In our view, a number of reasons explain the contradictory proposals that have been advanced for interpreting the peculiar behaviour exhibited by the M/CeO₂ catalysts upon increasing the reduction temperature. Some of these reasons are briefly commented on below.

1.2. *Proving the existence of strong metal/support interaction in M/CeO₂ catalysts – some experimental problems*

Among the chemical effects associated with the onset of the SMSI state in titania-supported metal catalysts, the practical suppression of chemisorption of the usual probe molecules, like H₂ or CO, is generally assumed to be a common characteristic feature [3,7]. By contrast, numerous hydrogen chemisorption studies on powder Rh/CeO₂ [7,30,80,81,83,95,101,107,119], and Pt/CeO₂ [16,30,49,150] catalysts suggest that, though the apparent H/M ratio generally decreases on increasing the reduction temperature, no complete inhibition of the H₂ chemisorption capability occurs upon reduction at 773 K, the typical temperature at which the SMSI state is induced in M/TiO₂ catalysts. As deduced from the H/M data reported in [30] for a series of M/CeO₂ (M: Ru, Rh, Ir,

Pd and Pt) catalysts reduced at both 473 and 773 K, this observation seems to be rather general. Moreover, significant hydrogen chemisorption still occurs on a Rh/CeO₂ catalyst reduced at 1000 K [81]. Contrary to that generally observed on M/CeO₂ catalysts, a few authors have reported strong deactivation of the H₂ adsorption capability of Rh/CeO₂ [83] and Ni/CeO₂ [145] catalysts reduced, respectively, at 773 and 673 K.

CO chemisorption has also been used for characterising M/CeO₂ catalysts. Some CO/M data are summarised in [19,26,35,125]. As already noted for the hydrogen chemisorption, the apparent CO/M values decrease with the reduction temperature but no drastic inhibition effects are generally observed. A rather similar conclusion could be obtained from the FTIR studies of chemisorbed CO on Pt/CeO₂ [16,21,54], Pd/CeO₂ [60,69], and Rh/CeO₂ [117]. In some cases [69], complete suppression of the CO chemisorption capability has also been suggested to occur.

Catalytic activity assays have also provided clear indications of the change of chemical properties occurring in M/CeO₂ catalysts on high-temperature reduction. Some of the most commonly investigated probe reactions were: hydrogenolysis of saturated hydrocarbons [16,22,43,119,151], and hydrogenation of benzene [7,16,63,145], acetone [119,125], CO [39,43,76,119,152], and CO₂ [30,95,98,119]. In the case of the hydrogenolysis, and benzene or acetone hydrogenation reactions, the high-temperature reduction treatment generally leads to deactivation effects of varying intensity. By contrast, the transient CO₂ hydrogenation experiments reported in [30,95,119] have revealed that the high-temperature reduced catalysts show an enhanced methanation activity. A rather similar effect was observed for the CO hydrogenation reaction [119]. Also remarkable, the enhanced transient activity was found to occur regardless of which metal, Ru, Rh, Ir, Pd or Pt, was investigated [30]. Under steady-state conditions, on the contrary, the high-temperature reduction treatment induces a moderate loss of activity for the CO and CO₂ hydrogenation reactions [30,95,119].

When the chemical effects induced on M/CeO₂ catalysts by the variation of the reduction temperature are analysed, it is important to note the likely occurrence of side-effects which may very much prevent the straightforward interpretation of the observed

changes. In this respect, it is worth recalling some of these effects. First of all, ceria is acknowledged to be an oxide with a relatively poor textural stability, particularly under reducing conditions [14,153,154]. Consequently, the often considered “high-temperature” reduction treatments (≥ 773 K), may induce strong support sintering. Associated with this primary effect, metal encapsulation and/or sintering phenomena may take place, and therefore, a catalyst deactivation effect would occur [107]. Also important, the contribution of this side effect to the observed deactivation can hardly be quantified. In spite of its presumably relevance, details about the textural evolution undergone by the M/CeO₂ catalysts on increasing the reduction temperature are often lacking [35,60,63, 83,119,151].

Proving the occurrence of metal deactivation effects is also complicated by the chemical side-processes occurring during the adsorption of the most usual probe molecules, like H₂ or CO. In the case of the hydrogen chemisorption studies, the likely occurrence of spillover phenomena represents a major drawback. As clearly shown by the magnetic balance studies performed on Rh/CeO₂ [115,116] and Pd/CeO₂ [61] catalysts, large amounts of hydrogen can be transferred to the ceria support, even at 298 K. Consequently, the apparent H/M ratios as determined from conventional chemisorption experiments may provide very misleading, highly overestimated metal dispersion data [107,155]. Moreover, it is well established that the contribution of the hydrogen spillover to the apparent H/M values is highly sensitive to a number of variables. Firstly, though the hydrogen chemisorption on ceria has been suggested to lead to a bronze-like phase by incorporation of hydrogen in the bulk [156], the results reported in [157] rather suggest that this process very probably consists of a purely surface reaction. If so, the intensity of the hydrogen spillover should be very sensitive to the ceria surface area. In good agreement with this statement, the maximum apparent H/Rh values (those determined after activating the spillover reaction) reported in [107] for two Rh/CeO₂ catalysts, with different surface area, was more than 10 times larger in the case of the high surface area sample. A second important factor influencing the spillover rate at 298 K is the reduction/evacuation conditions applied during the catalyst preparation. As shown by the magnetic balance study

reported in [101], and also in agreement with the chemisorption studies reported in [107], upon increasing the reduction/evacuation temperature from 623 to 773 K the spillover process becomes much slower. Accordingly, the comparison of the H/M values determined after low- and high-temperature reduction should be made carefully because of the different relative weight of the spillover contribution, presumably larger in the case of the low-temperature reduction. A third factor affecting the spillover phenomena is the use of chlorine-containing metal precursors. It is presently well established that, upon reduction, the chloride ions originating from the metal precursor are strongly retained by the support [63,70,80,92,94, 103,108,158]. In some cases, the presence in the reduced catalyst of crystalline CeOCl has been proved by means of XRD [63,70,158] and HREM [108]. The results reported in [80,107] strongly suggest that the presence of chlorine in the ceria support very much affects its hydrogen chemisorptive properties, thus having a negative influence on both the quantitative weight and rate of the spillover processes. Because of the generalised use of the chlorine-containing species as precursors of M/CeO₂ catalysts, the influence of this factor should always be considered when interpreting H₂ chemisorption data. There is however, a further element of complication; as suggested by the TPO-MS study reported in [92], the calcination of the precursor/ceria system prior to reduction may eliminate part of the chlorine initially present in the catalyst. Consequently, this oxidising pretreatment, which is often applied, though it probably does not lead to the complete removal of the chlorine [92] eliminates rather an unquantified part of it. Under these circumstances, the actual chlorine content of the M/CeO₂ catalysts is in most cases unknown.

The interpretation of the CO chemisorption data is not free from perturbing side-effects. In addition to the metal-dependent stoichiometric problems, it is now well known that ceria may also chemisorb large amounts of CO [19,60,66,67,125,159–161]. In addition, the amount of CO chemisorbed by ceria is sensitive to its redox state, it being generally acknowledged that this amount grows as the degree of reduction of ceria degree is increased [60,160]. Also, CO dissociation has been reported to occur on both the reduced bare oxide [162], and M/CeO₂ catalysts [86]. Finally, it is worth noting that, as in the case of the

hydrogen chemisorption, the use of chlorine-containing metal precursors may also disturb the CO adsorption on the support [66,80].

The analysis of the likely occurrence of strong metal/support interaction effects in M/CeO_2 catalysts also requires a good knowledge of the evolution undergone by the metal dispersion with the reduction temperature. However, as deduced from the results commented on above, the conventional H_2 and/or CO adsorption data do not allow, in general, a straightforward estimate of the metal dispersion. In this respect, low-temperature (191 K) hydrogen chemisorption may constitute an alternative to the conventional measurements at 298 K, because of the inhibition of the spillover process [107]. Nevertheless, a few studies are presently available [7,81,107,120]. Likewise, the specificity of the FTIR bands due to CO chemisorbed on the metal phase has allowed the development of an alternative procedure, which has been applied to determine the metal dispersion in ceria-supported Pt [54] and Pd [72] catalysts. In any case, it is obvious that the chemical techniques would provide very misleading dispersion data, if associated with the applied reduction treatment some metal deactivation would occur. It is therefore very desirable to have methods available for determining the metal dispersion in NM/CeO_2 catalysts other than those based on chemical techniques.

Though they were considered in the past to be of limited interest [54,72], the studies at present available have clearly shown that the high-resolution electron microscopy is one of the most powerful techniques for investigating the nanostructural constitution of ceria-supported metal catalysts [6,7,19,29,39,43,52,59,63,78,79,93,107,108,116,124,150,163]. In effect, as shown in [78,93] HREM allows us to establish the microcrystal size distributions, and therefore, the metal dispersion associated with the NM/CeO_2 (NM: noble metal) catalysts. This is an important information which provides reference data to be used in the interpretation of the chemical changes occurring in the catalyst when the reduction conditions are varied. In this respect, it is worth noting that, as deduced from the computer simulation studies reported in [78,79], there is a lower size limit for the detection of noble metal particles sitting on the ceria surface. This limit has been estimated to be 1.0 nm, so that the HREM would not allow accurate determinations of the metal

size distribution in very highly dispersed catalysts. In addition to the metal dispersion studies, the HREM technique has provided the very first direct experimental proof of metal decoration in Rh/CeO_2 [93], Pd/CeO_2 [63], and Pt/CeO_2 [29]. Likewise, it has allowed the occurrence of alloying phenomena in Pd/CeO_2 [59,63] and Pt/CeO_2 [29] to be established.

1.3. Determination of the ceria redox state in M/CeO_2 catalysts

As already noted, the occurrence of strong metal/support interaction effects is acknowledged to be associated with reduced states of the support. In accordance with this basic requirement, it is important to have detailed information about the redox evolution undergone by ceria when varying the reduction treatment. In the case of ceria-supported noble metal catalysts, this is also a challenging matter. Many different techniques have been used to probe the ceria redox state in both the bare oxide and NM/CeO_2 catalysts: ESR [84,125,164], XPS [20,80,83,90,96,122,158,165], electronic conductivity measurements [101,152], V–UV spectroscopy [13,166], FTIR spectroscopy [67,167], X-ray absorption spectroscopy (XAS) [103,158], and magnetic balance [13,14,61,92,94,101,115,116,168]. Likewise, oxygen consumption studies as determined by combining O_2 pulses at 298 K and TPO have also been fruitfully used to estimate the reduction degree of ceria in bare oxide [15], and in Rh/CeO_2 catalysts [100]. As the magnetic balance studies have clearly shown [61,101,115,116], when hydrogen is used as reducing agent, the analysis of the ceria redox state requires that two contributing factors are considered. In [94], they are referred to as reversible and irreversible components. The former would account for reduction contribution of hydrogen chemisorbed on ceria. This contribution can be eliminated by inducing the desorption of such species, so that the simple evacuation of the ceria-containing sample leads to its reoxidation. According to the results reported in [61,92,115,116], for high surface area NM/CeO_2 catalysts reduced at moderate temperatures ($T_{\text{redn}} \leq 623$ K), this contribution may represent about two-thirds of the total concentration of Ce^{3+} species present in the catalyst. The irreversible contribution would be associated with the oxygen vacancies created in the sample by the reduction

treatment. It may be determined by measuring the residual concentration of Ce^{3+} species after evacuation at sufficiently high temperature so as to ensure the complete elimination of the chemisorbed hydrogen [61,92,115,116], typically $T \geq 773$ K. As shown in [61,92,101], this second contribution increases with the reduction temperature. According to these results, the actual redox state of ceria is sensitive not only to the reduction temperature, but also to the specific evacuation conditions following the reduction treatment. Moreover, the presence of a highly dispersed metal may dramatically modify both the relative weight of the two reversible and irreversible contributions and also the specific hydrogen desorption behaviour of the M/CeO_2 catalyst with regard to evacuation conditions [101].

When analysing the ceria redox state in NM/CeO_2 catalysts, there is an additional, interesting aspect to be considered: the likely presence of chlorine in the oxide. As already noted, the reduction of the chlorine-containing precursor/ceria systems induces the incorporation of the chloride ions into the support structure [63,70,80,92,94,103,108,158]. When this occurs the magnetic balance studies reported in [92,94] show a dramatic change in the redox properties of ceria, which becomes heavily and irreversibly reduced even at the mildest reduction temperature, 623 K [92,94]. Accordingly, the presence of strongly held chloride ions completely blocks the reversibility of the redox behaviour of ceria, which is associated with hydrogen chemisorbed on the support, as discussed above. Though no specific data are available, this blocking effect probably depends on the amount of chlorine incorporated into the support, which in turn may be determined, among other factors, by the specific calcination treatment applied to the precursor/ceria system before reduction or the BET surface area of the ceria support.

The question is whether the concentration of oxygen vacancies is relevant to the onset of strong metal–support interaction effects in NM/CeO_2 catalysts. If so, we have to consider that there are two factors other than oxygen vacancies to be correlated with the total concentration of Ce^{3+} present in the catalyst samples: some forms of chemisorbed hydrogen and the presence of chloride ions.

1.4. Major objectives of this work

In this paper, we shall review some of the most recent results on the subject. The results to be discussed in this work were obtained on catalyst samples for which some of the problems mentioned above were minimised or eliminated. Essentially, the following basic ideas were taken into account in the catalyst selection: (a) when analysing chemical properties, the use of chlorine containing metal precursors was avoided; (b) the ceria supports were selected in such a way that within the range of experimental reduction temperatures, minor textural changes would occur; (c) the metal loading was also controlled so as to allow that the whole metal particle size distribution could be determined by means of HREM. In this way true metal dispersion data free from the problems associated with the conventional chemisorption techniques could be established.

In our approach, we shall first review the nanostructural information available at present. Then we shall analyse some chemical observations which, in our view, may shed some light on the actual nature of underlying physical phenomena. Finally, some concluding remarks will summarise the state of the art of the matter. In these considerations, the analogies and differences noted between M/CeO_2 and M/TiO_2 catalysts will be emphasised. Likewise, some differences observed between the most investigated supported metal phases: Rh, Pt, and Pd will also be commented on.

2. Experimental

The ceria-supported platinum and rhodium catalysts investigated here were prepared from two cerium dioxide samples, hereafter referred to as LS and MS oxides. The LS sample was a commercial oxide, from Alpha, with a low BET surface area ($4 \text{ m}^2 \text{ g}^{-1}$), and high textural stability: no measurable loss of surface area was observed after reduction in a flow of pure H_2 , for 1 h, at 973 K. The MS sample was prepared by heating a high surface area oxide ($135 \text{ m}^2 \text{ g}^{-1}$), at 823 K, for 4 h, in a flow of pure H_2 . The sample thus pretreated was further evacuated for 1 h in a flow of He, cooled to 298 K, also under flowing inert gas, and finally reoxidised with pure O_2 at 773 K (1 h). The

resulting cerium oxide shows no microporosity, a BET surface area of $34 \text{ m}^2 \text{ g}^{-1}$, and good textural stability for reduction treatments up to 773 K.

The preparation procedure was similar for all the catalysts. The noble metals were deposited onto the ceria supports by following the incipient wetness impregnation technique. Aqueous solutions of chlorine-free metal precursors: $[\text{Pt}(\text{NH}_3)_4](\text{OH})_2$ and $\text{Rh}(\text{NO}_3)_3$ were used. The impregnated samples were dried in air, at 383 K, for 10 h, and further stored in a desiccator until their reduction “in situ”.

The reduction treatments consisted of heating the precursor/support system in a flow of pure hydrogen, at a heating rate of 10 K min^{-1} . Reduction temperatures ranging from 473 to 1223 K were applied. For the Pt/CeO₂-MS catalysts the top limit reduction temperature was 773 K. The time of treatment at the selected reduction temperature was typically 1 h. The catalysts were further evacuated (1 h) at the reduction temperature, or at 773 K, if $T_{\text{redn}} \leq 773 \text{ K}$. In this work, results corresponding to three series of catalysts: Pt(4%)/CeO₂-LS, Pt(7%)/CeO₂-MS and Rh(2.4%)/CeO₂-LS will be presented and discussed.

The reoxidation experiments on the pre-reduced catalysts were performed by heating them in a flow of pure O₂ from 298 K to the selected temperature, at a heating rate of 10 K/min. The samples were kept at the reoxidation temperature for 1 h, and then cooled to room temperature, always under flowing O₂.

The HREM (high resolution electron microscopy) images were recorded on a JEOL 2000-EX instrument equipped with a top entry specimen holder and an ion pump. The structural resolution was 0.21 nm. The experimental protocol for transferring the samples to the microscope is reported elsewhere [93]. Digital processing of the recorded HREM images was carried out with the help of a high resolution CCD camera, COHU model 4910, and the SEMPER 6+ software package.

The TPD and H₂/D₂ exchange studies were performed in an experimental device coupled to a quadrupole mass spectrometer, VG, model SENSORLAB-200-D. In the case of the exchange studies, the reduced and/evacuated catalysts were treated with flowing H₂(5%)/Ar, at 298 K, for 15 min, then the gas flow was switched to D₂(5%)/N₂, and the transient period of the experiment (ITK: isotopic transient kinetic)

recorded. After 15 min of treatment under flowing D₂(5%)/N₂, at 298 K, the sample was cooled to 191 K also in a flow of the D₂/N₂ mixture. Finally, the gas flow was switched to Ar, and a TPD-MS experiment was run in two steps, from 191 to 298 K, and then from 298 to 773 or 1223 K. The typical amount of catalyst in all these experiments was 200 mg, the gas flow rate: $60 \text{ cm}^3 \text{ min}^{-1}$, and the heating rate: 10 K min^{-1} (298–1223 K). In the 191–298 K range, the heating of the catalyst samples occurred freely.

The experimental protocol described in the previous paragraph has also been followed in the case of the TPD-MS studies carried out on reduced/evacuated catalysts further treated with flowing pure hydrogen at different temperatures.

The hydrogen volumetric adsorption experiments were run in a conventional high vacuum system equipped with a capacitance gauge, MKS Baratron, model 220-BHS. The isotherms were recorded at 298 K, the time elapsed between successive adsorption measurements in routine was 20 min, and the final H₂ pressure 300 Torr. Following the conventional isotherm experiments, at 298 K, the samples were heated at several different temperatures (T_i), kept for 1 h at the selected T_i , and then cooled again to 298 K, always under hydrogen pressure (P_{H_2} at 298 K: 300 Torr). In this way the additional hydrogen consumption associated with the induced spillover process could be determined.

3. Nanostructural evolution of the NM/CeO₂ catalysts under both reducing and oxidising conditions – a HREM study

3.1. HREM study of the metal particle size distribution – determination of the metal dispersion

Though the number of the HREM studies on ceria-supported noble metal catalysts is rapidly growing [6,7,19,29,39,43,52,59,63,78,79,93,107,108,116,124,150,163,169,170], a few of them have paid special attention to the determination of the metal dispersion [78,93]. The approach followed in [78,93] consists of combining experimental HREM studies with digital processing of the experimental micrographs and computer simulation techniques. As an initial step, a metal

microcrystal model representative of those experimentally observed was established. By analysing hundreds of micrographs recorded in our laboratory for ceria-supported rhodium [7,78,79,93,100,107,108,170] and platinum [29,79,150] catalysts, the truncated cubo-octahedron was considered to be the most commonly observed metal morphology. This observation is also consistent with the experimental HREM images reported in the literature for Pt/CeO₂ [6,39,52] and Rh/CeO₂ [163,169] catalysts. Likewise, the proposal is supported by the good matching observed between the experimental images and those obtained by computer calculations made on the basis of our structural model [78,79]. Fig. 1 allows the comparison of both the experimental and calculated HREM images corresponding to a Rh/CeO₂ catalyst. The structural model used as input in the computer simulations is also depicted in Fig. 1.

In accordance with the now well-known structural relationships occurring at the NM/CeO₂ interface [6,7,18,59,78,107,169], the model metal particle has

been built up in such a way as to allow that its (1 1 1) basal plane sits on a (1 1 1) surface plane of the ceria support. Following this assumption, the basal plane of the metal particle shown in Fig. 2 is obtained. Accordingly, the metal microcrystal size was measured by means of the parameter d in Fig. 2. As described in further detail in [78], the equations developed by Van Hardeveld and Hartog [171] then allow the size (d) to be used to estimate the metal dispersion, i.e. N_s/N_t , where N_s and N_t stand, respectively, for the total number of metal atoms and the number of surface atoms in the metal particle.

Regarding the use of the HREM technique in metal dispersion studies, it is important to note that, as shown in [172], the physical processes associated with the formation of HREM images may induce an apparent distortion in the images of nanosized particles. In [78], the relevance of this effect was investigated by analysing computer simulated images which were generated from models of ceria-supported model rhodium particles of known size. Though the distortion

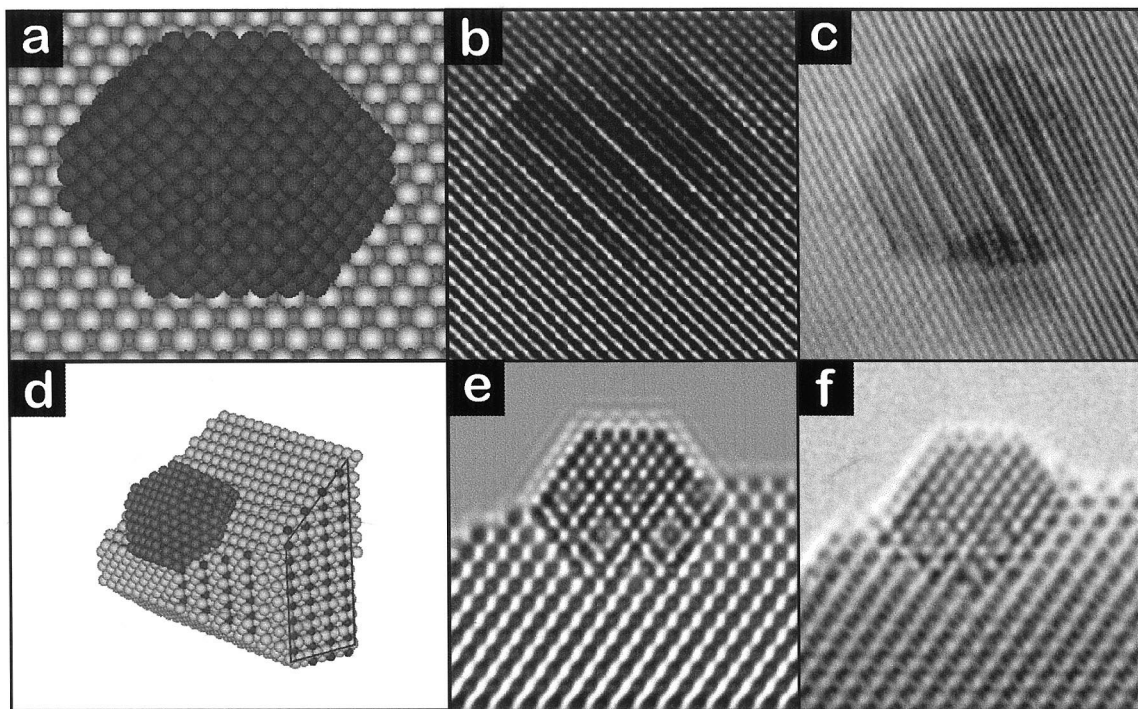


Fig. 1. Experimental (c and f) and computer simulated (b and e) HREM images for a Rh(2.4%)/CeO₂-LS catalyst, planar (b and c) and profile (e and f) views. The metal particle model consisting of a truncated cubo-octahedron with (1 1 1) basal plane sitting on a (1 1 1) surface plane of ceria is also shown along the [1 0 0] (a) and [1 1 0] (d) zone axis of Rh. Taken from [78].

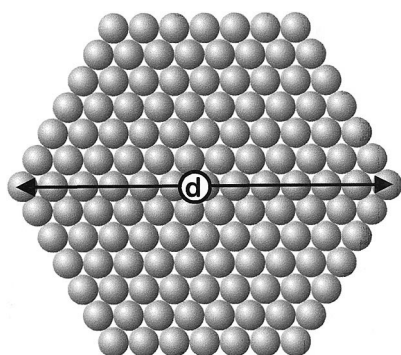


Fig. 2. (111) basal plane of the truncated cubo-octahedron metal particle used as a model for determining metal dispersions in NM/CeO₂ catalysts. The geometrical parameter (*d*) measures the particle size. Taken from [78].

phenomena were observed, they are within the experimental error in the particle size measurements, and therefore allow meaningful metal dispersion data to be obtained [78].

Computer simulation techniques have also been used to establish the lower limit in the HREM detection of Rh particles supported on ceria [79,93]. Microcrystals observed in profile [79,93] and planar [93] views were considered in these computer simulations. In both cases the detection limit was estimated to be about 1.0 nm, thus suggesting that HREM should be carefully used for characterising very highly dispersed catalysts. In this particular case, the technique may underestimate the true metal dispersion values.

Based on the particle model described above, the measurement of the size (*d*) of some hundreds (typically more than 250) of metal microcrystals, which was performed on tens of HREM micrographs, allows three types of distribution curves to be constructed, as shown in Fig. 3. These three distribution curves account for the variation of: the cumulative percentage of metal particles (type A); the cumulative percentage of the total number of metal atoms contained in particles with size equal or smaller than a predefined size (type B), or the percentage of the total number of metal atoms that are present at the surface of particles with size equal or smaller than a predefined value (type C), with the metal particle size. All of them provide interesting information about the distribution of the metal particles [79]. Metal dispersion data may be obtained either from type C plots, or from the mean size metal particle values as determined from A-type

plots. As shown in [79], significant differences may be observed between both kinds of dispersion data, the former providing the most accurate estimate of this parameter. Accordingly, data reported in Table 1 were all obtained from type C plots.

In accordance with the results summarised in Table 1, for reduction temperatures up to 773 K, the metal sintering effects are very moderate on both CeO₂-LS and CeO₂-MS supported metal catalysts. Higher reduction temperatures were only studied on the LS series of catalysts. For $T_{\text{redn}}=973$ K, the loss of metal dispersion is significantly larger in the case of platinum. This observation is remarkable because the metal loading, if expressed as number of metal atoms per nm² of support, is slightly larger in the case of Rh, and no measurable support sintering could be detected on any of the two catalysts. Therefore, our results suggest that the Pt stability against sintering is poorer than that of Rh. For Pd/CeO₂, the results reported in [63] suggest that the evolution of the metal microcrystal mean size with the reduction temperature is similar to that observed on our Pt/CeO₂ catalyst. In effect, for the catalyst prepared from a chlorine-free metal precursor (palladium nitrate), on increasing the reduction temperature from 573 to 773 K, the mean Pd microcrystal size (d_m) as determined by XRD was found to increase from 14 to 15 nm, the sintering effect being much stronger after reduction at 973 K: $d_m=28$ nm. As deduced from the mean size data commented on above, however, the catalysts investigated in [63], with high metal loading (9%), and unknown surface area, exhibit much poorer dispersion than ours. Likewise, their standard reduction time (20 h) was much longer than ours (1 h).

The influence of the reoxidation treatments on the metal dispersion also deserves some comments. As deduced from Table 1, reoxidation at 773 K has only slightly detrimental or no effect on the metal dispersion. Regarding the high-temperature (1173 K) reoxidation treatment, which was applied to the most heavily reduced catalysts (1173 K), the HREM images reported in Section 3.2.2 of this work show the occurrence of metal microcrystals smaller than those existing in the starting high-temperature reduced catalysts. Nevertheless, as will be commented on further in Section 3.2.2, at least in the case of the Pt/CeO₂-LS catalyst, very large metal particles coexist with the small ones, thus suggesting a strong bimodal

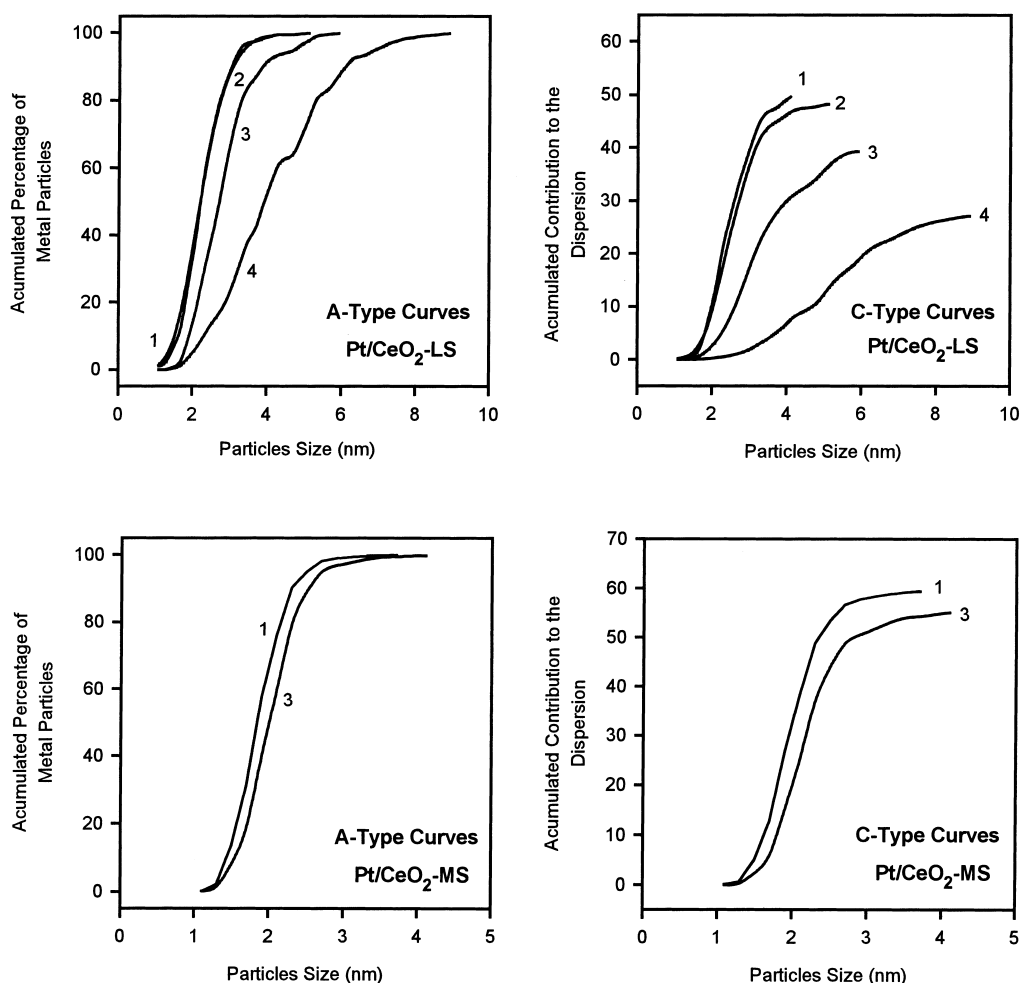


Fig. 3. Types A and C metal size distribution curves corresponding to Pt(4%)/CeO₂-LS and Pt(7%)/CeO₂-MS catalyst reduced with flowing H₂ (1 h) at the indicated temperatures: 473 K (1), 623 K (2), 773 K (3) and 973 K (4).

distribution which does not allow a precise estimate of the metal dispersion.

3.2. HREM study of the nanostructural evolution undergone by the NM/CeO₂ systems treated at increasing temperatures under both reducing and oxidising conditions

3.2.1. Studies on the NM/CeO₂ catalysts reduced at temperatures ranging from 473 to 1223 K

3.2.1.1. Catalysts reduced with flowing H₂ The number of studies dealing with the TEM/HREM

characterisation of NM/CeO₂ catalysts has significantly grown in the last few years [6,7,19,29,39,43,52,59,63,77–79,93,100,107,108,116,124,150,163,169]. Upon reviewing the literature available, we may notice that all these studies have been performed on catalysts reduced with H₂. Likewise, a major fraction of them were focussed on catalyst samples reduced at temperatures not higher than 773 K [6,7,19,39,43,52,77,107,116,124,163,169]. Though no specific reasons have been given to justify the election of this upper limit reduction temperature, it seems to be likely that the choice was influenced by the reference character of 773 K as typical reduction

Table 1
HREM study of the metal dispersion ($D=100 \times N_s/N_t$) in a series of Pt/CeO₂ and Rh/CeO₂ catalysts pretreated as indicated below

Catalyst	T_{redn} (K)	Further treatment	D (%)
Pt (4%)/CeO ₂ -LS	473	–	50
Pt (4%)/CeO ₂ -LS	623	–	49
Pt (4%)/CeO ₂ -LS	773	–	40
Pt (4%)/CeO ₂ -LS	973	–	27
Pt (4%)/CeO ₂ -LS	773	Reoxn. 773 K (1 h)+evac.. 773 K (1 h)+Redn 623 K (1 h)	38
Pt (7%)/CeO ₂ -MS	473	–	60
Pt (7%)/CeO ₂ -MS	773	–	56
Pt (7%)/CeO ₂ -MS	773	Reoxn. 773 K (1 h)+evac.. 773 K (1 h)+Redn 623 K (1 h)	53
Rh (2.4%)/CeO ₂ -LS	623	–	46
Rh (2.4%)/CeO ₂ -LS	773	–	38
Rh (2.4%)/CeO ₂ -LS	973	–	36
Rh (2.4%)/CeO ₂ -LS	1173	–	16
Rh (2.4%)/CeO ₂ -LS	1173	Reoxn 773 K (1 h)+evac.. 773 K (1 h)+Redn 623 K (1 h)	16
Rh (2.4%)/CeO ₂ -LS	1173	Reoxn 1173 K (1 h)+evac.. 773 K (1 h)+Redn 623 K (1 h)	39

Data determined from Type C distribution curves like those shown in Fig. 3.

temperature inducing the onset of the SMSI state in M/TiO₂ catalysts [3]. Moreover, the use of the NM/CeO₂ catalysts as model systems for investigating TWCs strongly suggests the interest of studying their behaviour at temperatures well above 773 K [173]. All these observations prompted us to initiate an in depth HREM study aimed at investigating the nanostructural evolution undergone by a series of Pt/CeO₂ and Rh/CeO₂ catalysts when submitted to reduction treatments varying over a wide range of temperatures, from 473 to 1173 K. Parallel HREM studies on Pd/CeO₂ reduced at temperatures well above 773 K have also been recently published [59,63].

In our view, the widening of the range of reduction temperatures has been critically important for better understanding of the actual nature of the metal/support interaction phenomena occurring in ceria based catalysts.

Fig. 4 shows some representative HREM micrographs corresponding to Pt/CeO₂ and Rh/CeO₂ catalysts reduced at 773 K or lower temperatures. As deduced from the images in profile view, the metal microcrystals all appear clean and well faceted. This observation, which has already been noted in earlier papers from our laboratory [7,19,29,93,107,108,150], is also in full agreement with several other HREM studies on Pt/CeO₂ [6,52] Pd/CeO₂ [59,63], and Rh/

CeO₂ [163,169]. This is the first noteworthy conclusion from all the HREM studies at present available: in contrast with results reported for M/TiO₂ [4,5,6,7], on NM/CeO₂ catalysts (NM: Pd, Pt, Rh), the hydrogen reduction treatments at temperatures up to 773 K do not induce covering of the metal microcrystal by the reduced support. Though not proved, several authors have speculated about the role played by the metal decoration effects in the deactivation of M/CeO₂ catalysts reduced at 773 K or below [60,69,117, 119,125,145]. The HREM data reasonably allow us to exclude such a possibility.

The HREM studies on NM/CeO₂ catalysts reduced at $T_{\text{red}} \leq 773$ K, however, have proved the existence of well-defined metal/support structural relationships. The very first experimental evidence of such a relationship was reported by Cowley et al. [18], who on the basis of nanodiffraction studies performed on a Rh/CeO₂ catalyst reduced at both 623 and 773 K proposed the occurrence of a parallel alignment of metal and support $[h k l]$ axes with the same Miller indices. In [18], experimental nanodiffraction patterns showing parallel Rh/CeO₂ orientations in $[1 1 1]$ and $[1 0 0]$ directions were reported. Later on, several HREM studies on Rh/CeO₂ [7,79,93,107,169], Pt/CeO₂ [6], and Pd/CeO₂ [59] have given further support to this proposal. Also in good agreement with them, all the HREM images presented in Fig. 4 clearly show the

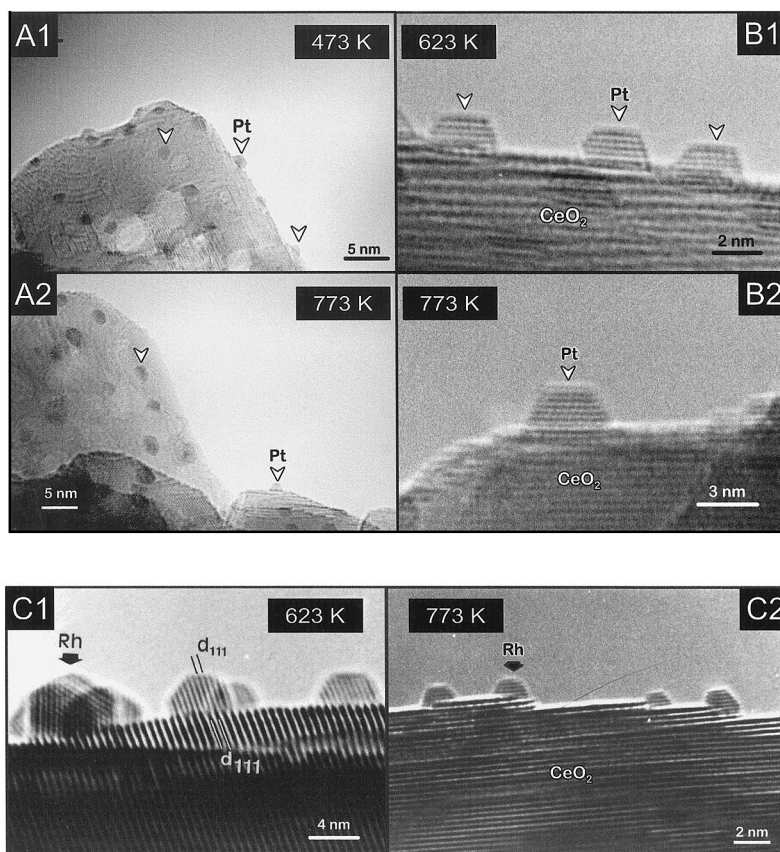


Fig. 4. HREM study of the nanostructural constitution of a series of ceria supported Pt and Rh catalysts reduced with H_2 at different temperatures up to 773 K. Profile view images corresponding to: (A) Pt(7%)/CeO₂-MS; (B) Pt(4%)/CeO₂-LS; (C) Rh(2.4%)/CeO₂-LS. The specific T_{redn} are indicated on the micrographs. All the catalysts were prepared from chlorine free metal precursors.

parallel growth of (1 1 1) planes of the metal, Pt or Rh, on (1 1 1) planes of the ceria supports. A detailed analysis of the structural relationships occurring in Rh/CeO₂ catalysts has been recently reported [93]. In this work, the combined analysis of experimental and computer simulated HREM images has allowed the existence of two different epitaxial relationships to be established. In both cases the metal/support interface consisted of Rh(1 1 1) and CeO₂(1 1 1) in parallel orientation. For the first type of epitaxy, which was referred to as (1 1 1)/(1 1 1) 0°, all the [h k l] axes of metal and support are in parallel orientation (parallel epitaxy). By contrast, the second type would formally result from a 60° rotation around the [1 1 1] axis of a Rh microcrystal with all its crystallographic axes in parallel orientation with those of the support. Because of the sixfold symmetry of the (1 1 1) planes, this

rotation would lead to an equivalent Rh/CeO₂ interface, but several [h k l] axes of the metal and support would become misaligned. In accordance with this formal description, the second epitaxial relationship was referred to as (1 1 1)/(1 1 1) 60° (twin epitaxy) [93]. Fig. 5 summarises both experimental and computer simulated HREM images showing the two types of epitaxial relationships commented on above. Also worth noting, the double diffraction phenomena (moiré patterns) generated by the metal microcrystals when viewed in planar projection on the support have been fruitfully used in the analysis of the epitaxial relationships occurring in NM/CeO₂ [6,59,93].

The HREM study of the NM/CeO₂-LS catalysts reduced at 973 K, Fig. 6, indicates the occurrence of remarkable nanostructural changes. In addition to the effects on the metal microcrystal size distributions,

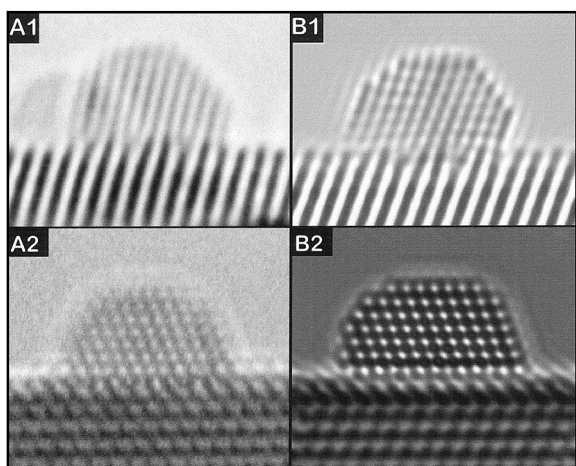


Fig. 5. Experimental (A) and computer simulated (B) HREM images corresponding to the observed Rh/CeO₂ structural relationships. In [93], they are referred to as: (1) parallel epitaxy (1 1 1)/(1 1 1)0°; and (2) twin epitaxy (1 1 1)/(1 1 1)60°. The experimental images were obtained on a Rh(2.4%)/CeO₂-LS catalyst reduced with H₂ (1 h), at 623 K.

already commented on, a new outstanding feature may be observed: the partial covering of the metal particles by a very thin, a few angstrom thick, layer of a different phase. It was deduced from the application of digital processing and computer simulation techniques [93], that the overlayer actually consists of ceria. As seen in Fig. 6, metal decoration effects do occur on both Rh and Pt catalysts. A statistical analysis of several tens of experimental micrographs has shown that about 30% of the Rh microcrystals were decorated, the percentage being significantly larger, 70%, in the case of the Pt catalyst. Also worth noting is that the HREM images in Fig. 6 suggest that the migration of the reduced ceria to the top of the metal microcrystals, rather than the burial of the metal particles into the ceria bulk, is the most likely decoration mechanism.

HREM has also provided clear evidence of metal covering effects in Pd/CeO₂ [59,63]. On a catalyst prepared from PdCl₂, decoration was found to occur after 20 h reduction at 873 K [63]; a rather similar effect was observed on a sample prepared from Pd(NO₃)₂, after 20 h reduction at 973 K [59]. In the latter case, however, no results corresponding to the catalyst reduced at 873 K were reported.

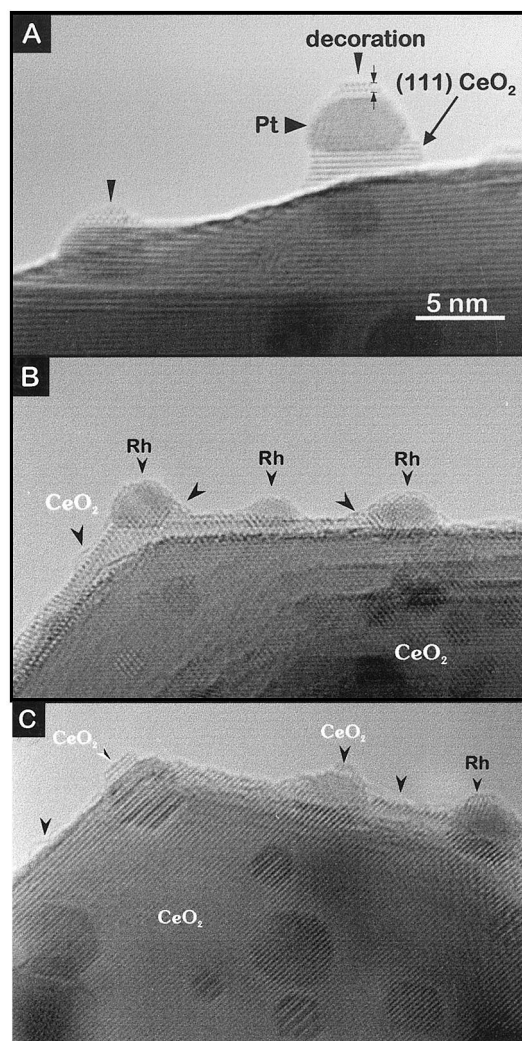


Fig. 6. HREM study of the metal decoration effects occurring in Pt(4%)/CeO₂-LS reduced at 973 K (A), and in Rh(2.4%)/CeO₂-LS catalyst reduced at 973 (B) or 1173 K (C).

The effect of very high-temperature reduction treatments, 1173–1223 K, has also been investigated on Rh/CeO₂ [93], Pt/CeO₂ [29] and Pd/CeO₂ [59]. In accordance with the HREM data now available, there are notable differences of behaviour from one noble metal to the other.

Fig. 7 shows HREM images corresponding to Rh and Pt catalysts reduced at 1173 K. In the case of the Rh(2.4%)/CeO₂-LS sample, the contrasts observed in all the recorded micrographs may be interpreted as due to rhodium and ceria [93]. Compared with the catalyst

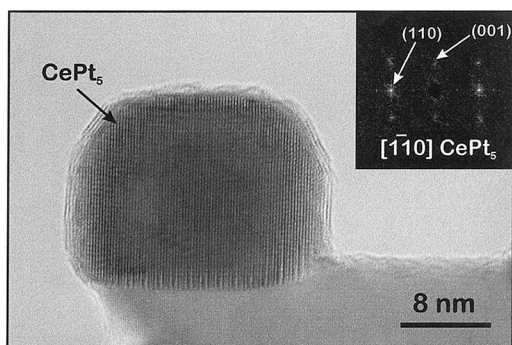


Fig. 7. HREM study of the Pt(4%)/CeO₂ catalyst reduced with H₂ (1 h), at 1173 K. The inset digital diffraction pattern (DDP) shows that the particle marked with an arrow in the micrograph consists of a Pt₅Ce microcrystal in [1–3,4,5,6,7,8,9,10] orientation.

reduced at 973 K, Fig. 6(C), the most significant nanostructural differences are: the shift of the Rh size distribution towards higher values [78,93]; the increase of the fraction of decorated metal crystallites, from 30% up to 90%; and the enhanced crystallinity of the ceria overlayers. No evidence of alloying phenomena could be deduced from these studies.

In the case of Pt(4%)/CeO₂-LS catalyst reduced at 1173 K (1 h), particles showing peculiar HREM contrasts other than those corresponding to either Pt or CeO₂ could be observed, Fig. 7(b). As discussed in [29], these contrasts may be unequivocally interpreted as due to the CePt₅ phase. The presence in the catalyst of the CePt₅ alloy phase could also be confirmed by XRD. Moreover, in accordance with the crystallographic characteristics of the five well-known Pt–Ce intermetallic compounds: CePt, CePt₂, Ce₃Pt₂, Ce₇Pt₃ and CePt₅ [174,175–177], it could be established that the CePt₅ phase was the only one present in the catalyst [29]. This alloy phase is the same as that observed by XRD on heating a physical mixture of Pt black and CeO₂, under H₂, at 1173 K [178]. Though not proved, the formation of the CePt₅ phase has also been proposed to be responsible for the deactivation observed on a Pt/CeO₂ catalyst reduced at 773 K [16]. The results commented on here, however, suggest as very unlikely the occurrence of alloying phenomena after reduction at such a relatively moderate temperature.

The statistical analysis of the micrographs recorded for the Pt/CeO₂ catalyst reduced at 1173 K also shows that 80% of the Pt mass is in the form of alloy

microcrystals, the remaining 20% consisting of pure metal [29]. Also the alloy crystallites appear decorated by a thin layer of support, Fig. 7(b). Though not unequivocally proved, this ensemble of HREM observations commented on above suggests that, upon increasing the reduction temperature, the nanostructural evolution of the supported platinum phase takes place through three steps. During the first one, for $T_{\text{redn}} \leq 773$ K, the catalyst would consist of well-faceted, undecorated metal particles. After reduction at 973 K, about two-thirds of the metal crystallites would be partly covered by the support. Finally, at $T_{\text{redn}}=1173$ K, a deep reduction of ceria with inherent transformation of the decorated Pt crystallites into overlayers CePt₅ alloy particles with a CeO₂ overlayer would take place.

In the case of Pd/CeO₂ [59,63], alloying phenomena have also been proposed to occur. Compared with the results commented on above for Pt/CeO₂, however, there are some significant differences. Even on the catalyst reduced for 20 h, at the highest temperature, 1180 K, the authors [59] were unable to detect by either XRD, SAED or HREM any stoichiometrically well-defined Pd–Ce phase. By contrast, on the basis of their XRD study, they propose the formation of a solid solution of Ce in the Pd lattice [59]. As discussed in [63], this solid solution would also exhibit an f.c.c. structure, the only difference with pure Pd being its slightly larger (2.3%) lattice parameter. In accordance with their XRD studies, the alloy phase starts to be observed upon reduction at a temperature as low as 773 K [63], it becoming the majority phase after reduction at 873 or 973 K [59,63]. Though the reduction times routinely applied in [59,63] are longer than usual, which would certainly favour formation of the alloy, there are some striking aspects in these observations. Firstly, the microstructure of the catalysts, with 9% metal loading, and unknown BET surface area, is very peculiar. Even at the lowest reduction temperature, 573 K, they consist of very large metal crystallites: 14.0 nm “supported” on a ceria sample with a mean crystal size of 11.0 nm [59]. After reduction at 773 K, the crystallite size of both metal and support increases significantly, 17.4 nm for Pd, and 15.4 nm for CeO₂, becoming much larger on reduction at 973 K, 27.6 and 28.5 nm, respectively. These data suggest the existence of a small metal/support interface, which would not favour the proposed solid state

reaction between them. Secondly, the authors report rather similar findings on both the ex-chloride and ex-nitrate catalysts. In the former case, however, a CeOCl phase coexists with ceria [63]. The question is how this second phase, probably present at the surface of the support, would modify the redox properties of ceria. In this respect, it is worth noting, that a HREM study performed in our laboratory on a Pt (2.4%)/ CeO_2 -LS sample prepared from hexachloroplatinic acid has demonstrated that, upon reduction at 1173 K (1 h), no Pt_5Ce phase is formed. This suggests that the presence of chlorine disturbs the alloying process. To summarise, though the results reported in [59,63] may reasonably be interpreted as an indication of the capability of the Pd/ CeO_2 system to easily form an alloy phase, some additional microanalytical and structural proofs would probably be required to confirm such a proposal.

3.2.1.2. Catalysts reduced with flowing CO
Compared with the studies in which hydrogen is used as the reducing agent, those dealing with the reduction with CO of either bare ceria [154,168] or ceria containing metal catalysts [55,104,179] should be considered as a minority. In spite of this, the investigation of the nanostructural evolution undergone by the NM/ CeO_2 catalysts under CO reducing atmosphere should be considered highly interesting, particularly, in connection with their use as TWC model systems. Accordingly, we have carried out a HREM study on a Pt(4%)/ CeO_2 -LS catalyst reduced with flowing CO(5%)/He, at 773 K (1 h). Fig. 8 shows some representative HREM images corresponding to this catalyst. As deduced from them, the use of diluted CO as reductant, even at moderate temperatures, leads to the formation of heavy carbonaceous deposits, which in accordance with the HREM images seem to grow surrounding the metal crystallites. This observation, which obviously precludes the realisation of a nanostructural investigation parallel to the one performed on the hydrogen-reduced catalysts, gives, however, further support to earlier studies dealing with Rh deposited on $\text{CeO}_2(111)$ and $\text{CeO}_2(100)$ surfaces [86,90]. As discussed in [86], the oxygen vacancies at the ceria surface would play an important

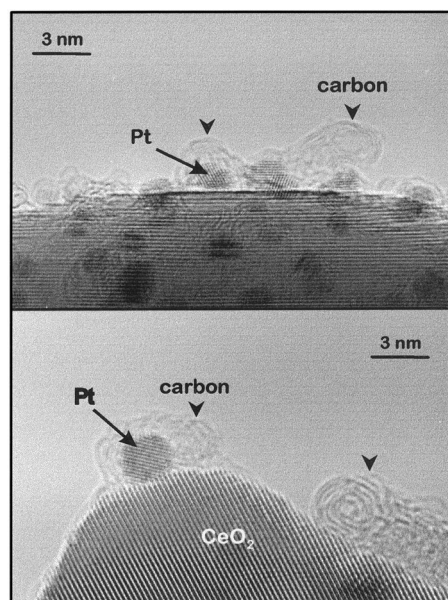


Fig. 8. HREM images showing the amorphous carbon deposits formed on the surface of the Pt(4%)/ CeO_2 -LS catalyst upon reduction with flowing CO(5%)/He at 773 K (1 h).

role in the activation of the CO dissociation process, a correlation being established between the support reduction degree and the fraction of chemisorbed CO undergoing dissociation. These observations suggest that the thermal evolution of our Pt/ CeO_2 catalyst under flowing CO would probably take place through two successive steps. In accordance with several previous studies on Pt/ CeO_2 [21,180], Pd/ CeO_2 [55,62], and Rh/ CeO_2 [90,104], the first step might well imply the irreversible reduction of the support, with inherent creation of oxygen vacancies at the ceria surface. During the second one, the CO dissociation would occur on the Pt/ CeO_{2-x} catalyst.

3.2.2. Nanostructural characterisation of the reoxidised NM/ CeO_2 catalysts

The investigation of the chemical and nanostructural effects associated with the reoxidation of a supported metal catalyst which is supposed to be under a SMSI-like state, is generally considered to provide an essential piece of information for unequivocally establishing the occurrence of such an effect [1,3]. Accordingly, a systematic HREM study has been performed in this direction. Both Pt/ CeO_2 -LS and Rh/ CeO_2 -LS [78,93,100] catalysts reduced at 773,

973 and 1173 K have been investigated. Likewise, several reoxidation temperatures ranging from 373 to 1173 K were applied.

In the case of M/TiO₂ systems, it is generally acknowledged that reoxidation at 773 K followed by a mild reduction treatment allows to recover these catalysts from the SMSI state [1,3,8]. Consequently, 773 K may be considered as a reference reoxidation temperature in the investigation of the SMSI-like phenomena. We shall pay special attention to this treatment. Moreover, several authors [6,21,43,69, 119] working on “high-temperature” (673–773 K) reduced NM/CeO₂ catalysts have already applied this sort of reoxidation treatments. In the specific case of the results presented here, all the catalysts were reoxidised with flowing O₂, at 773 K, for 1 h.

Fig. 9 presents some HREM images corresponding to the Rh/CeO₂-LS reduced at 773 and 1173 K and further reoxidised at 773 K. As expected from earlier studies on the rhodium oxidation [181,182–184], the rounded particles shown in Fig. 9 actually consist of polycrystalline Rh₂O₃. This proposal was supported by the oxygen consumption data as determined from O₂ Pulses/TPO experiments on the reduced catalysts [100]. Likewise, the digital diffraction patterns (DDP) recorded for the oxidised particles are in agreement with it [93,100]. These DDPs are inset in Fig. 9.

The Rh/CeO₂-LS samples resulting from the reduction at 623 K of the reoxidised catalysts were also investigated. From the analysis of the corresponding micrographs some interesting conclusions could be drawn [78,93]. Firstly, the dispersion data reported in Table 1 show that this reoxidation treatment does not significantly modify the metal dispersion. Secondly, upon comparison of the HREM images reported in Fig. 6(C) and Fig. 9(C), we may conclude that the nanostructure of the metal particles in both the catalyst directly reduced at 1173 K, Fig. 6(C), and that of the metal particles resulting from its reoxidation at 773 K, and further reduction at 623 K, Fig. 9(C), is different. In effect, the re-reduced catalyst, Fig. 9(C), shows rounded polycrystalline particles, instead of the decorated well-defined Rh microcrystals observed after direct reduction at 1173 K, Fig. 6(C). Also interesting is the analysis of the DDP inset in Fig. 9(C) that shows the coexistence of both Rh and CeO₂ microcrystals [93]. This would indicate that the applied reoxidation treatment, though inducing significant nanostructural

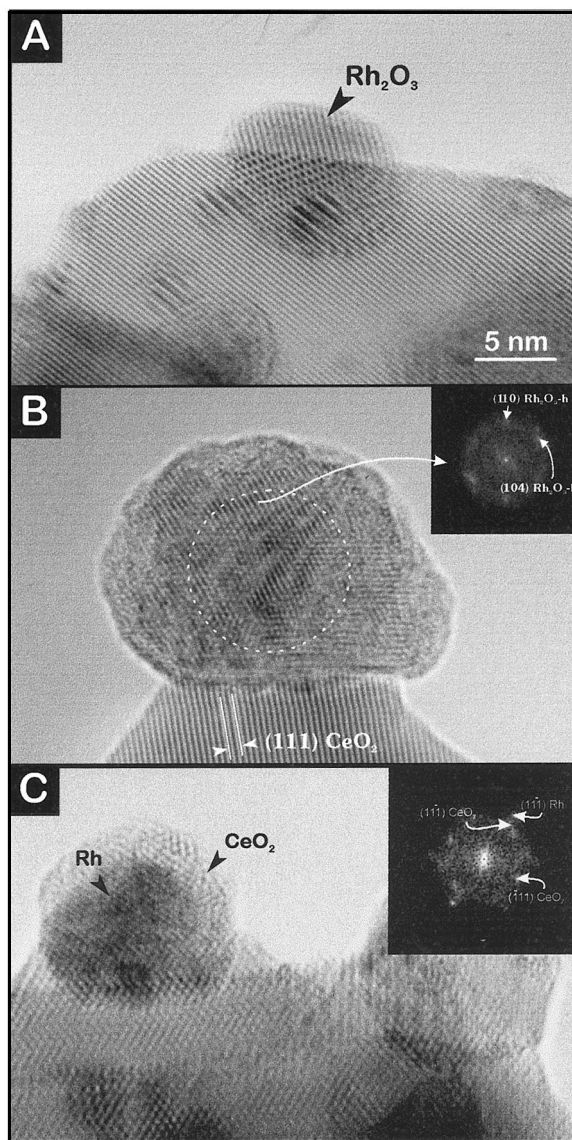


Fig. 9. HREM images corresponding to the Rh/CeO₂-LS catalyst reduced at 773 K (A), and 1173 K (B), and further reoxidised with flowing O₂, for 1 h, at 773 K. Also included is a micrograph of the reoxidised sample B, further reduced at 623 K (C). Digital diffraction patterns (DDPs) of selected regions of the images are shown as insets.

changes, does not allow to recover the catalyst from the original decoration effects. This behaviour clearly contrasts with that exhibited by the NM/TiO₂ catalysts [6,8].

In the case of the Rh/CeO₂-LS catalyst reduced at 973 K, because of the significant presence of both decorated and undecorated metal particles, the behaviour against the reoxidation at 773 K may be considered in between those reported in Fig. 9 for the catalysts reduced at either 773 or 1173 K.

HREM studies have also been performed on the Rh/CeO₂-LS catalyst reduced at 1173 K and further reoxidised at 373, 573 and 1173 K [93]. The experimental protocol was similar to the one applied in the case of the reoxidation studies at 773 K. As discussed in [93], reoxidations below 773 K lead to decorated partly oxidised rhodium particles, no change of the metal particle size distribution or recovery from decoration being observed in any case. By contrast, the reoxidation at 1173 K leads to clean well-faceted Rh microcrystals, with parallel redispersion of the metallic phase [78]. In effect, as shown in Table 1, the metal dispersion associated with the catalyst reoxidised at 1173 K, 39%, is much larger than that of the sample reduced at 1173 K, 16%, becoming closer to that of the catalyst directly reduced at 623 K, 46%.

Rather similar reoxidation studies have been performed on the Pt(4%)/CeO₂-LS catalyst reduced at 773, 973 and 1173 K. In contrast with that reported for Rh/CeO₂, crystallographically well-defined platinum oxides could not be observed. The external faces of the oxidised metal particles look like rounded exhibiting poor contrasts, Fig. 10(A). The diffuse borders of the Pt particles are interpreted as due to the outer oxidation of the metal crystallites. Accordingly, the HREM studies were usually performed on catalysts further re-reduced at 623 K, Fig. 10(B). In accordance with the dispersion data reported in Table 1, the oxidation at 773 K followed by re-reduction at 623 K does not significantly modify the metal dispersion of the catalyst directly reduced at 773 K.

Fig. 11 shows HREM images corresponding to the Pt/CeO₂-LS catalyst reduced at either 973 or 1173 K, further reoxidised at 773 K (1 h), and finally reduced at 623 K (1 h). As deduced from this figure, large rounded particles of the metal containing phases are observed. DDPs like that inset in Fig. 11(B) show that in both cases, i.e. the decorated (T_{redn} : 973 K) and alloy (T_{redn} : 1173 K) crystallites, the resulting oxidised particles actually consist of aggregates of Pt and CeO₂ microcrystals. This would indicate that, as already noted for Rh/CeO₂, the reoxidation treatment

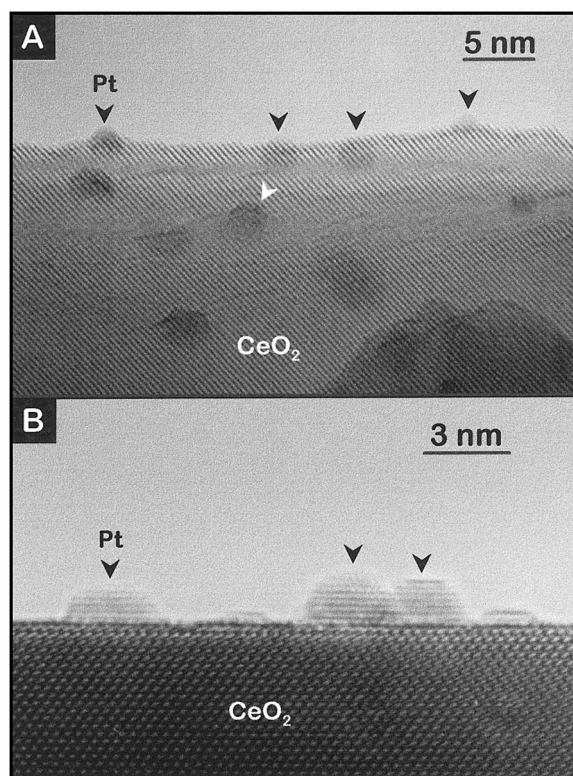


Fig. 10. HREM images corresponding to the Pt(4%)/CeO₂-LS catalyst reduced at 773 K and: (A) further reoxidised at 773 K; and (B) reoxidised at 773 K and further reduced at 623 K.

at 773 K does not allow to recover the Pt/CeO₂ catalysts from decoration or alloying phenomena.

The Pt/CeO₂ catalyst reduced at 1173 K was also reoxidised at 1173 K (1 h), and finally re-reduced at 623 K. As shown in Fig. 12, small clean well-faceted platinum particles could be observed in the HREM images. It should be noted, however, that, after reoxidation, the density of metal crystallites was significantly lower than that observed on the catalyst directly reduced at $T_{\text{redn}} \leq 773$ K. This suggests the occurrence of a heavy bimodal distribution of the platinum, or some metal loss. In this latter respect, either diffusion of the oxidised platinum into the ceria bulk, or some transfer of oxidised species to the gas phase may explain this observation. To clarify this particular point, a new high-metal-loaded catalyst, Pt(9%)/CeO₂-LS, was prepared by following the same procedure as that used in the case of the Pt(4%)/CeO₂-LS sample. This new catalyst was studied by using a

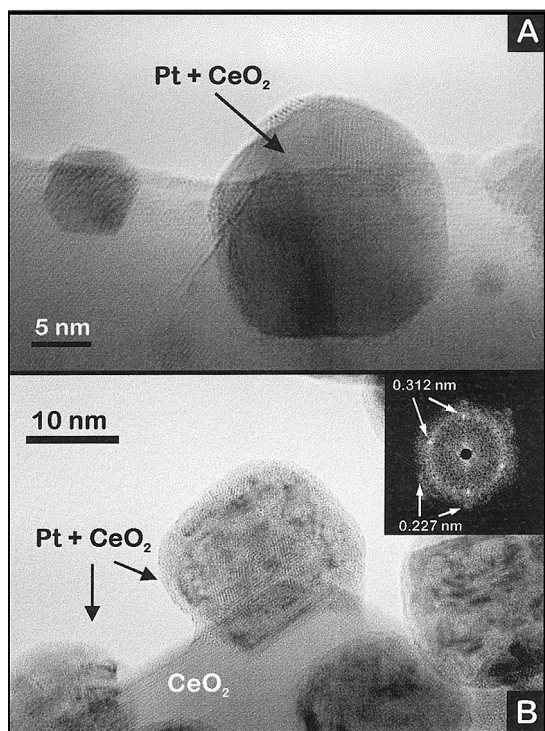


Fig. 11. HREM images corresponding to the Pt(4%)/CeO₂-LS catalyst reduced at 973 K (A) and 1173 K (B), further reoxidised at 773 K (1 h), and finally reduced at 623 K (1 h).

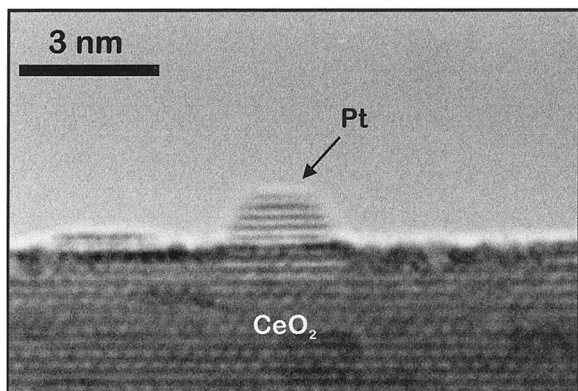


Fig. 12. HREM study of the Pt(4%)/CeO₂-LS catalyst reduced at 1173 K (1 h), further reoxidised at 1173 K (1 h) and finally reduced at 623 K (1 h).

scanning electron microscope (SEM) equipped with microanalytical (EDS) facilities. In spite of its limited analytical resolution (1 μm), dot mapping analysis carried out on the sample reduced at 773 K and further reoxidised at 1173 K allowed the identification of very

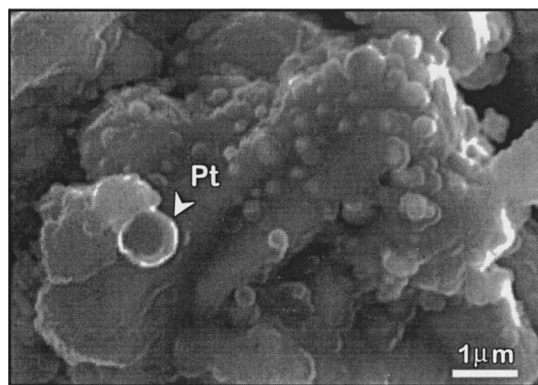


Fig. 13. SEM/EDS study of the Pt(9%)/CeO₂-LS catalyst reduced at 773 K, and further reoxidised at 1173 K. The arrowed metal particle could be identified by means of dot EDS microanalysis.

large metal particles, in the order of 1 μm , Fig. 13. This would indicate that the high-temperature reoxidation treatment induces a bimodal distribution leading to such large Pt particles that can hardly be identified by using HREM. Moreover, the HREM images recorded for the Pt(4%)/CeO₂-LS catalyst reduced at 1173 K, and further reoxidised at the same temperature, Fig. 12, shows the presence of platinum crystallites smaller than those usually found in the sample directly reduced at 473 K. This indicates that, under high-temperature oxidising conditions, the operating sintering mechanism probably consists of an atom migration from the small platinum crystallites to the larger ones. Associated with this mechanism a bimodal particle size distribution should be expected to occur [185]. Also interesting is the dot mapping analysis of large catalyst areas (1000 $\mu\text{m} \times 700 \mu\text{m}$) performed on both the catalyst reduced at 773 K and that resulting from its reoxidation at 1173 K, that indicated that the Pt/Ce ratio was 60% smaller in the latter case, Fig. 14. Since EDS provides bulk analytical information (Depth analysis: 1 μm), the observed loss of platinum would reasonably be attributed to its transfer to the gas phase, rather than to bulk diffusion phenomena.

4. Chemical properties of the NM/CeO₂ catalysts reduced at increasing temperatures – effect of very mild reoxidation treatments

The influence of the reduction temperature on the chemical properties of the ceria-supported noble metal

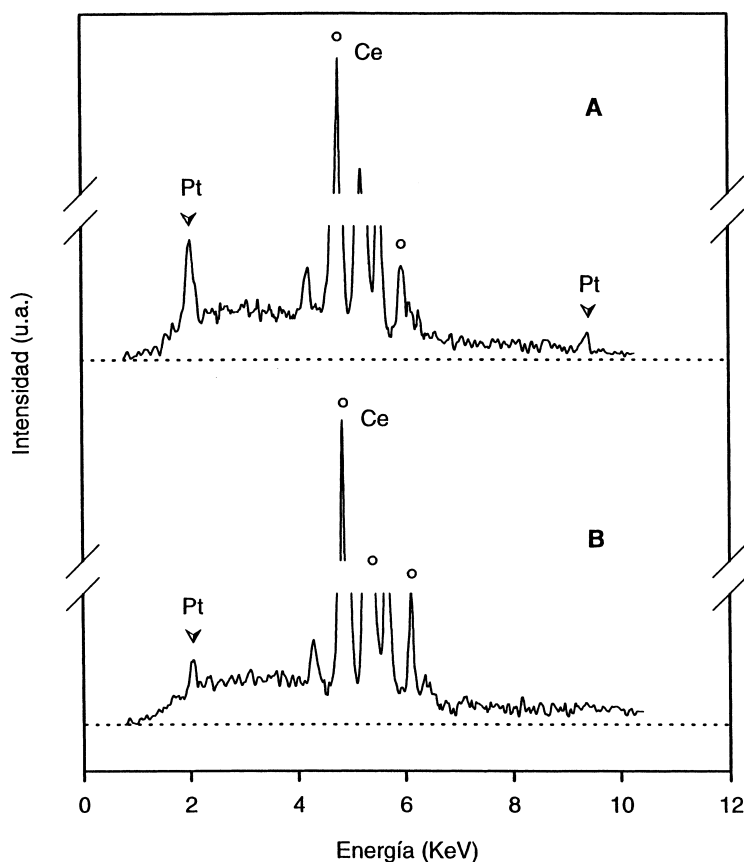


Fig. 14. EDS spectra recorded for the Pt(9%)/CeO₂-LS catalyst: (A) reduced with flowing H₂ at 773 K (1 h); and (B) reoxidised with flowing O₂ at 1173 K (1 h), after reduction at 773 K. The dot mapping analysis was performed on a large catalyst area: 1000 μm × 700 μm.

catalysts will be analysed on the basis of some recent studies dealing with the interaction of H₂ with the Pt(7%)/CeO₂-MS catalyst reduced at 473 or 773 K. It would be recalled that this catalyst was prepared from a chlorine-free metal precursor, and that the texture of the ceria support was pre-stabilised, thus ensuring no significant metal loss due to encapsulation effects. The HREM studies have also shown that the metal dispersion does not significantly change with the reduction treatment. Finally, the analysis of the HREM images have not revealed any evidence of metal decoration and alloying phenomena on the catalyst reduced at 773 K. The selected catalyst is, in summary, an ideal sample for investigating the changes that occurred in the chemical properties of the Pt/CeO₂ system on increasing the reduction temperature.

The results corresponding to the study of the H₂ interaction with the Pt(7%)/CeO₂-MS catalyst will be presented and discussed in Sections 4.1 and 4.2, the former will deal with the volumetric adsorption and temperature-programmed desorption (TPD-MS) data; whereas in the latter, we shall report on the H₂/D₂ exchange studies.

4.1. Hydrogen volumetric adsorption and TPD-MS studies on Pt(7%)/CeO₂-MS catalysts reduced at increasing temperatures

In accordance with the experimental protocol established earlier for Rh/CeO₂ [107], the volumetric chemisorption studies were performed as follows: the catalyst reduced at 473 or 773 K was further evacuated at 773 K for 1 h, and a conventional hydrogen

Table 2
Volumetric study of the hydrogen chemisorption on the Pt(7%)/CeO₂-MS catalyst

Treatment ($T_{\text{redn}}/T_{\text{evac}}$)	Apparent H/Pt (K)			
	298	373 ^a	473 ^a	623 ^a
473/773 K	0.61	0.91	1.03	–
773/773 K	0.19	0.42	0.77	0.82

^aAmount of chemisorbed H₂ as determined at 298 K after activating the spillover process by heating the sample under H₂ pressure (P_{H_2} at 298 K:300 Torr), for 1 h, at the indicated temperature, and further cooling to 298 K always under hydrogen pressure.

isotherm was recorded at 298 K. Then, the spillover process was activated by heating the sample at several increasing temperatures. In every case, the catalyst was held for 1 h at the selected temperature, and finally cooled to 298 K, always under hydrogen pressure. The amounts of hydrogen chemisorbed after each of these experiments are reported in Table 2. As justified in [107], the H/Pt values summarised in Table 2 were determined from the last experimental point of the corresponding isotherm (P_{H_2} : 300 Torr), without any further correction.

The TPD-MS studies were performed by following an experimental protocol resembling that earlier applied to some Rh/CeO₂ catalysts [19,101,120]. After reduction at 473 or 773 K, for 1 h, the catalyst was evacuated in a flow of He, at 773 K, for 1 h, cooled to room temperature, also in a flow of the inert gas, then treated with flowing pure H₂, for 1 h, either at 298 K, or at several increasing temperatures. Always in a flow of H₂, it was further cooled up to 191 K, then the flowing gas was switched to He, and, finally the TPD was run. The TPD-MS experiments were recorded in two steps, from 191 to 298 K, low temperature, and from 298 K onwards, high temperature. Fig. 15 shows the diagrams corresponding to the high-

temperature step. The apparent H/Pt values presented in Table 3 were determined by integration of the traces recorded throughout both the low- and high-temperature TPD steps.

The results reported in Tables 2 and 3 show a very good agreement between the volumetric and TPD data. Thus, for the adsorption studies at 298 K, the H/Pt values in Table 2 0.61 (T_{redn} : 473 K), and 0.19 (T_{redn} : 773 K), are very close to those reported in the last column of Table 3 (TPD-MS studies): 0.61 and 0.21, respectively. These latter values account for the total amount of desorbed hydrogen, i.e. the contributions of both, low- and high-temperature steps of the TPD experiment, have been taken into account. In our view, the use of uncorrected H/Pt values in Table 2 suggests as the most reasonable alternative their comparison with the total H/Pt data in Table 3.

If the H/Pt values determined at 298 K are compared with the HREM metal dispersion data: 60% (T_{redn} : 473 K) and 56% (T_{redn} : 773 K), Table 1, we may conclude that the adsorption capability of the Pt(7%)/CeO₂-MS catalyst reduced at 773 K, though not suppressed, is significantly disturbed. This may be considered as the very first indication of some kind of metal deactivation effect. The observed decrease in

Table 3
Apparent H/Pt values as determined by integration of the TPD-MS traces recorded for the Pt(7%)/CeO₂-MS catalyst reduced at 473 or 773 K and further treated as indicated (see the text and the legend of Fig. 15 for further details)

T_{redn} (K)	Further H ₂ treatment	Apparent H/Pt		
		TPD (191–298 K)	TPD (298–773 K)	Total
473	Evac. 773 K/H ₂ 298 K/Cooling H ₂ 191 K	0.15	0.46	0.61
473	Evac. 773 K/H ₂ 473 K/Cooling H ₂ 191 K	0.13	0.92	1.05
773	Evac. 773 K/H ₂ 298 K/Cooling H ₂ 191 K	0.06	0.15	0.21
773	Evac. 773 K/H ₂ 473 K/Cooling H ₂ 191 K	0.04	0.68	0.72
773	Evac. 773 K/H ₂ 773 K/Cooling H ₂ 191 K	0.05	0.97	1.02

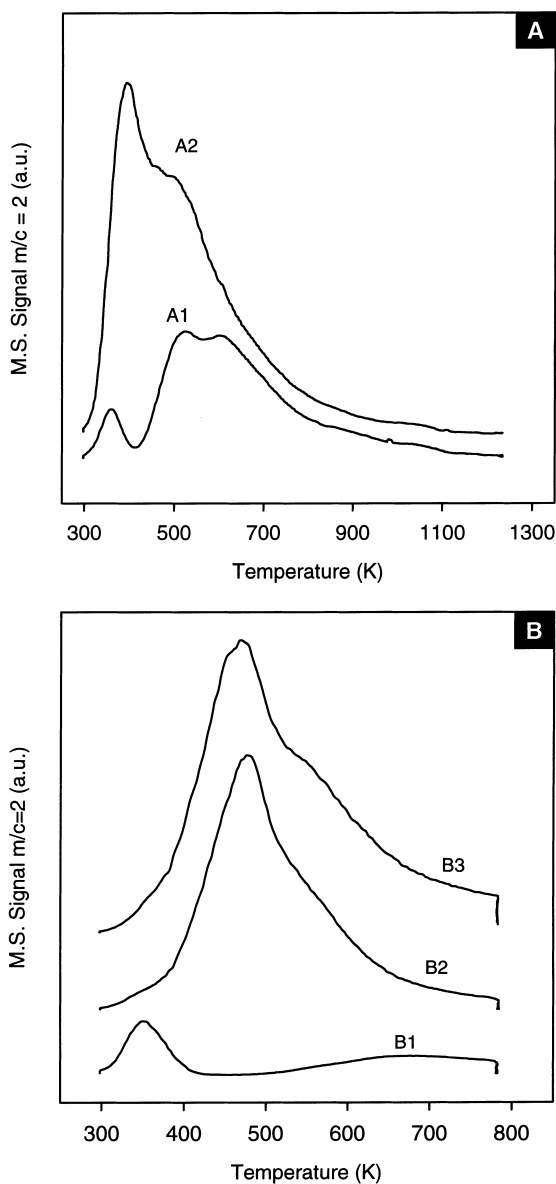


Fig. 15. TPD-MS study of the H_2 desorption from Pt(7%)/CeO₂-MS catalysts reduced at: (A) 473; (B) 773 K. After reduction, the samples were evacuated at 773 K (1 h) in a flow of He, followed by a further treatment with flowing H_2 (1 h) at the selected temperature (T_t), then the catalysts were cooled up down to 191 K (solid/liquid acetone cold trap), and finally the TPD-MS diagrams were recorded in two steps: from 191–298 K (free heating of the sample), and from 298 K upwards (heating rate: 10 K min⁻¹). The selected T_t values were: 298 K (traces: A1 and B1); 473 K (traces: A2 and B2); and 773 K (trace B3). The reported diagrams correspond to the second step of the TPD experiments.

the H/M ratio with the reduction temperature is in good agreement with earlier results for Pt/CeO₂ [16,30,31,43], and several other NM/CeO₂ [30,61, 119,132] catalysts. It would be noted, however, that in most of these previous studies, several relevant parameters, like those dealing with the nature of the metal precursor, or the textural and nanostructural evolution undergone by the catalyst on increasing the reduction temperature were not specially controlled.

In the hydrogen chemisorption studies on NM/CeO₂, the spillover contribution should always be evaluated. As already commented on, the spillover rate at 298 K is sensitive to the reduction/evacuation conditions, becoming slower as the reduction temperature is increased [101]. In the case of Pt(7%)/CeO₂-MS sample, this may also be the case. Thus, as shown in Table 2, the heating under H_2 pressure, at 373 K, induces an increase of H/Pt values slightly larger on the sample reduced at 473 K. Likewise, the A1 and B1 TPD diagrams in Fig. 15 also indicate some differences of behaviour between the catalysts reduced at 473 and 773 K. In effect, these TPD diagrams correspond to the catalysts evacuated first at 773 K and then treated with H_2 at 298 K. Accordingly, the hydrogen chemisorbed onto the support was eliminated prior to the further treatment with H_2 . As the temperature is raised during the TPD experiment, the spillover is activated, thus enabling the occurrence of the transfer of hydrogen from the metal to the support [101]. Under these conditions, the peak occurring below 400 K is interpreted as due to hydrogen directly desorbed from the metal, whereas the features appearing above 400 K would be assigned to hydrogen transferred first from the metal to the support, and then spilt over back in a through-the-metal process taking place at higher temperatures. As deduced from Fig. 15, both, the fraction of the total desorbed hydrogen involved in the reversible transfer between metal and support, and the temperatures at which the back-spillover is observed, suggest that these processes are faster on the catalyst reduced at 473 K.

Tables 2 and 3 provide some further information about the role played by the spillover phenomena. On the catalyst reduced/evacuated at 773 K, and further treated with H_2 at 773 K, the total amount of desorbed hydrogen was found to be: H/Pt=1.02, Table 3. If the total H/Pt value determined at 298 K, 0.21, is attrib-

uted to the metal, the difference, H/Pt:0.81, may be assigned to hydrogen chemisorbed onto the support. This value is in fairly good agreement with that determined from a TPD experiment in which the CeO₂-MS sample was reduced at 773 K (1 h) and further cooled to 191 K under flowing H₂. In this latter case, the amount of desorbed hydrogen is 157 μmole H₂ g⁻¹. If referred to nm² of the oxide surface area, a value, 6 H atoms nm⁻², close to the highest amount of hydrogen chemisorbed on ceria [15] is obtained. If expressed as equivalent H/Pt in the Pt(7%)/CeO₂-MS sample, the resulting value would be 0.78. We may conclude, accordingly, that the treatment with H₂ at 773 K leads the Pt/CeO₂ catalyst to a situation in which the support is practically saturated with hydrogen. If a parallel estimate is made for the catalyst reduced at 473 K, evacuated at 773 K, and then treated with H₂ at 473 K, the amount of hydrogen chemisorbed onto the support would be equivalent to H/Pt: 0.44. Though the likely contribution of the spillover to the H/Pt value determined at 298 K (0.61) has been ignored in this estimate, the difference existing with respect to the limit value (H/Pt:0.81), may reasonably be interpreted as indicative of a support far from the saturation. It would be concluded, accordingly, that the spillover process is relatively slow, even in the catalyst reduced at 473 K. In this respect, it is worth recalling that the surface hydroxyl groups seem to play an important role in determining the spillover rate [115,116,186,187], and that our Pt/CeO₂ catalysts were all evacuated at 773 K, after reduction. Under such evacuation conditions ceria becomes heavily dehydroxylated [15,107, 156,160]. To summarise, in the case of the Pt/CeO₂ samples investigated here, the spillover probably represents a minor contribution to the total amount of hydrogen chemisorbed at 298 K, even for the catalyst reduced at 473 K. If it were the case, the corresponding H/Pt values would mainly account for the chemical properties of the supported platinum.

The amounts of hydrogen desorbed throughout the low-temperature (191–298 K) step of the TPD experiments also deserve some comment. As shown in Table 3, the H/Pt data for the samples reduced at 473 and 773 K are significantly different from each other. By contrast, for the catalyst reduced at a given temperature, the H/Pt values are rather insensitive to the specific H₂ adsorption treatment. Since in the

temperature range of these TPD experiments the back-spillover, if occurs, should reasonably represent a minor contribution, and no peak could be observed in parallel studies on the bare support, we propose that the low-temperature desorption feature is due to hydrogen forms weakly chemisorbed on the metal. Assuming this interpretation, and taking also into account that the HREM has not revealed any major nanostructural change in the supported metal crystallites, the decrease of the H/Pt ratio from 0.13–0.15 for the catalyst reduced at 473 K, to 0.04–0.06, for the sample reduced at 773 K, might well be considered as an additional indication of the occurrence of some partial deactivation of the Pt microcrystals in the catalyst reduced at 773 K.

The changes observed in the desorption traces depicted in Fig. 15(A2) and Fig. 15(B3) (or B2) are also worth noting. For the catalyst reduced at 473 K, the highest desorption peak in trace A2 is observed at 393 K, the maximum shifting upwards up to 470 K on the sample reduced at 773 K (trace B3 or B2). Though some alternative interpretations are certainly possible, the shift above suggests that the contribution of the hydrogen giving rise to the peak at about 393 K, which may reasonably be assigned to species directly desorbed from the metal, is significantly smaller after reduction at 773 K. A TPD-H₂ diagram rather similar to the one depicted in Fig. 15(B3) has been reported for a Pt(2.02%)/CeO₂ catalyst reduced at 773 K and further cooled to 298 K, under H₂ [49]. In this latter case, however, H₂[PtCl₆] was used as metal precursor. For Pt(4%)/CeO₂-LS, the TPD-H₂ traces also show an analogous evolution with the reduction temperature, Fig. 16. Likewise, the TPD-H₂ diagrams for a high surface area (130 m² g⁻¹) ceria-supported rhodium catalyst reduced at 623 [120] or 773 K [101] are in good agreement with the trend commented on above. It seems, therefore, that the influence of the reduction temperature on the chemical properties of different NM/CeO₂ catalysts is a rather common effect.

4.2. Influence of the reduction temperature on the chemical behaviour of Pt/CeO₂ catalysts as revealed by H₂/D₂ exchange experiments

The nature of deactivation effects has also been investigated by means of H₂/D₂ exchange studies performed on the Pt(7%)/CeO₂-MS sample. Fig. 17

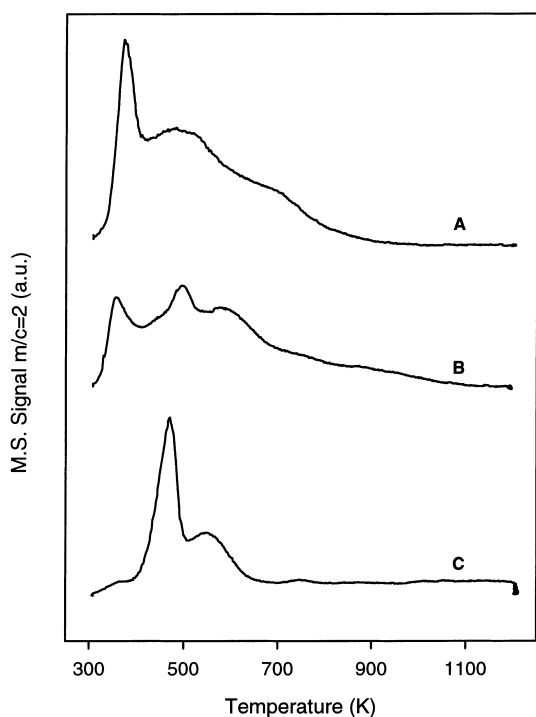


Fig. 16. TPD-MS study of the H_2 desorption from $Pt(4\%)/CeO_2$ -LS. The samples were reduced in a flow of hydrogen, for 1 h, at (A) 623, (B) 773, (C) 973 K, and further cooled always under flowing H_2 .

shows the traces recorded during the transient period of these exchange experiments. The catalyst reduced at either 473 or 773 K, further evacuated at 773 K, and cooled to 298 K under flowing Ar, was treated at room temperature with $H_2(5\%)/Ar$ for 15 min, then switching the gas flow to $D_2(5\%)/N_2$. All the experimental conditions: the H_2 (D_2) partial pressure (38 Torr), the temperature (298 K), and the time of treatment with $H_2(5\%)/Ar$ prior exchange (15 min), were selected with the aim of minimising the role played by the spilt over species during the transient period. Also worth noting, as deduced from Fig. 17, is that the exchange reactions mainly occur during the very first minute of the ITK experiment. Taking into account all these considerations, we may conclude that the transient traces would mainly, if not exclusively, account for the behaviour of the supported metal phase.

As deduced from the analysis of Fig. 17, the chemical properties of the platinum are drastically modified by the reduction conditions. For the catalyst reduced at 473 K, the transient traces clearly show the desorption of both H_2 , HD species. By contrast, after reduction at 773 K, H_2 desorption is almost completely suppressed, HD becoming the only product of exchange. Likewise, the reduction temperature modifies the shape of the transient traces for HD, thus indicating the existence of significant differences in

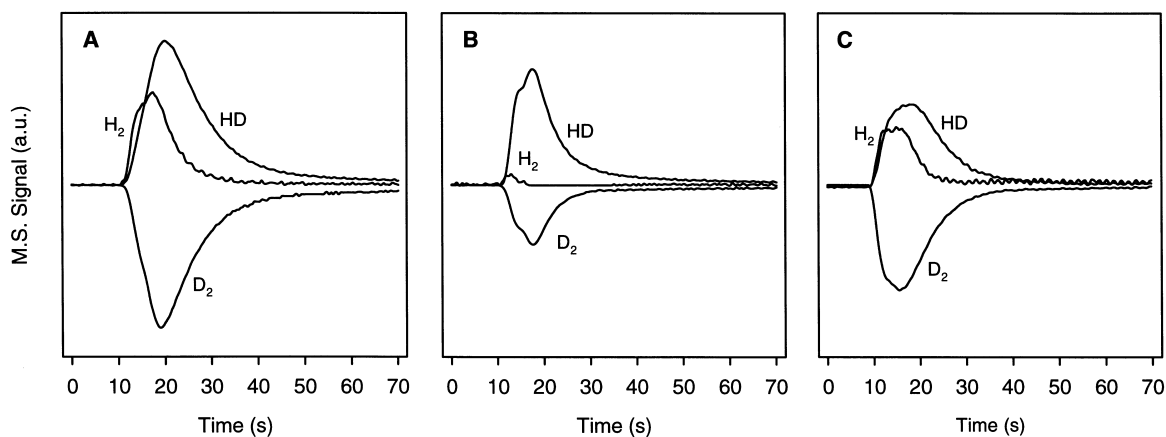


Fig. 17. Isotopic transient kinetic (ITK) experiments performed on the $Pt(7\%)/CeO_2$ -MS catalyst: (A) reduced with flowing H_2 at 473 K (1 h), then evacuated at 773 K (1 h) in a flow of Ar, cooled to 298 K under flowing Ar, further treated with flowing $H_2(5\%)/Ar$ for 15 min; finally, the gas flow was switched to $D_2(5\%)/N_2$. (B) The same experimental protocol, except $T_{redn}: 773$ K. (C) The catalyst reduced at 773 K was further reoxidised with flowing O_2 at 298 K (1 h), then treated with flowing $H_2(5\%)/Ar$ at 298 K (1 h), and further evacuated at 773 K under flowing Ar. The experiment was completed by following the protocol described for the sample A.

Table 4

Influence of the reduction temperature on the area under the transient traces for H₂, HD and D₂ reported in Fig. 17

Treatment	Area H ₂ (a.u.)	Area HD (a.u.)	Area D ₂ ^a (a.u.)
Redn 473 K/evac. 773 K/ITK 298 K	4.3	10.4	-9.3
Redn 773 K/evac. 773 K/ITK 298 K	0.3	6.1	-3.7
Redn 773 K/evac. 773 K/reoxn 298 K/ITK 298 K	2.7	5.5	-6.6

Traces corresponding to the H₂/D₂ exchange experiments performed on Pt(7%)/CeO₂-MS.^aThe negative values indicate deuterium consumption.

the kinetics of the exchange processes. A detailed analysis of the results presented in Fig. 17 will be reported elsewhere [188].

Upon integration of the traces for H₂, HD and D₂ in Fig. 17, an estimate of the relative amounts of H₂/D₂ exchanged during the transient period could also be made. Table 4 summarises the corresponding data as measured by the areas under the different ITK traces. The quantitative results reported in Table 4 confirm the chemical perturbations occurred on the Pt/CeO₂ catalyst. In effect, on the sample reduced at 773 K, the amount of exchanged hydrogen is less than 50% of that determined for the catalyst reduced at 473 K. As already noted, the relative change is particularly important in the case of the hydrogen species being desorbed as H₂.

A parallel H₂/D₂ exchange study has also been performed on the Pt(6.3%)/SiO₂ (EUROPT-1) catalyst, Fig. 18. Two main reasons justify the use of the EUROPT-1 in the present study. Firstly, it is a well characterised reference catalyst exhibiting a metal dispersion, 63%, very close to that of the Pt(7%)/CeO₂-MS [189,190–193]. Secondly, silica is generally considered as a non-reducible support. Accordingly, within the range of reduction temperatures applied here, the EUROPT-1 may account for the typical behaviour of a non-SMSI catalytic system. As deduced from the comparison of Figs. 17 and 18, the influence of the reduction temperature on the behaviour of the Pt/SiO₂ and Pt/CeO₂ catalysts is clearly different. In the first case, negligible effects are observed. By contrast, on Pt/CeO₂, the increase of the reduction temperature from 473 to 773 K induces both kinetic and quantitative changes in the behaviour of the catalyst. As already indicated, these effects should be interpreted in terms of the changes that occurred in the chemical properties of the supported platinum microcrystals.

Obviously, the results reported in Table 4 account for the exchanged hydrogen, not for the total amount present in the catalysts. This latter information is also relevant for establishing the occurrence of a true metal deactivation effect. Consequently, after completing the exchange experiment, the samples were cooled to 191 K under flowing D₂(5%)/N₂, then, the gas flow was switched to Ar, and the corresponding two-steps TPD-MS experiments were run. Fig. 19 shows the traces for H₂, HD and D₂ recorded in the 298–773 K desorption range. Upon integration of the corresponding TPD-MS signals, the amounts of H₂, HD and D₂, always expressed as equivalent H/Pt ratio could be determined, Table 5. Data for HD and D₂ were corrected by the corresponding sensitivity factors determined experimentally. The signal for H₂ was taken as reference. A good agreement between the results included in Tables 3 and 5 may be noted.

It is well known that the NM/CeO₂ catalysts prepared from chlorine-free metal precursors may be easily reoxidised with O₂, even at room temperature [92,94,103]. Likewise, the HREM studies reported here have shown that the reoxidation treatments below 773 K induce minor nanostructural effects on the Pt/CeO₂ and Rh/CeO₂ catalysts. Accordingly, it seemed interesting to perform an additional experiment aimed at checking the effect of a very mild reoxidation treatment on the chemical properties of a Pt(7%)/CeO₂-MS sample pre-reduced at 773 K. The catalyst was contacted with flowing O₂ at 298 K (1 h), then flushed with inert gas at 298 K, treated with H₂(5%)/Ar, for 1 h, also at 298 K, evacuated under flowing Ar at 773 K, treated again with H₂(5)/Ar for 15 min, at 298 K, and exchanged with D₂(5%)/N₂ following the routine described above. Fig. 17(C) shows the corresponding transient traces for H₂, HD and D₂. In accordance with them, the reoxidation treatment at

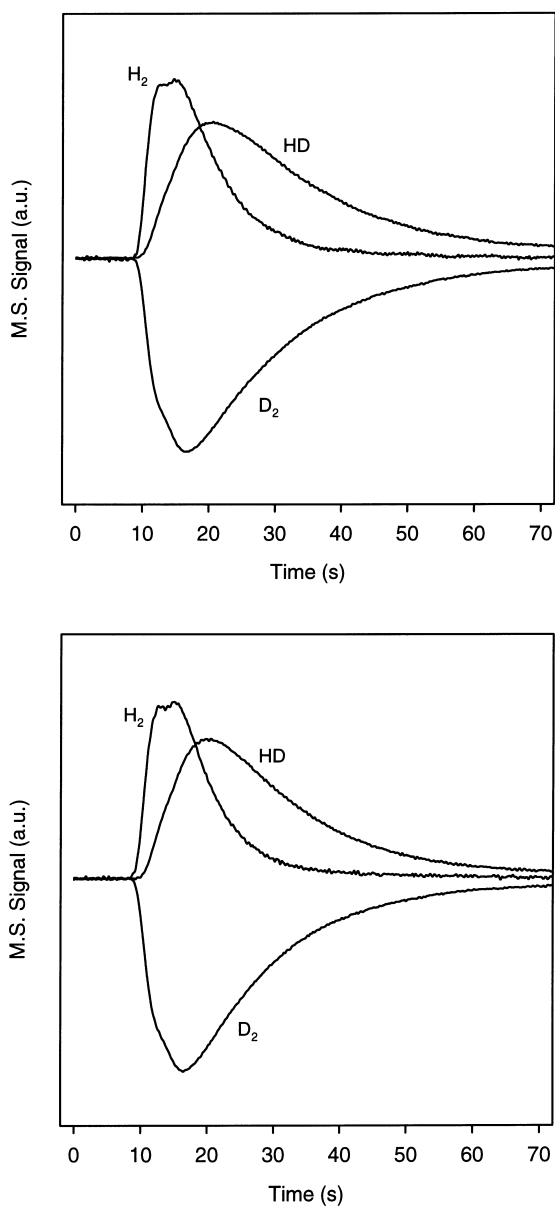


Fig. 18. Isotopic transient kinetic (ITK) experiments performed on the Pt(6.3%)/SiO₂ (EUROPT-1) catalyst: (A) reduced with flowing H₂ at 623 K (1 h), then evacuated at 773 K (1 h) in a flow of Ar, cooled to 298 K under flowing Ar, further treated with flowing H₂(5%)/Ar for 15 min; and finally, the gas flow was switched to D₂(5%)/N₂. (B) The same experimental protocol, except T_{redn} : 773 K.

298 K remarkably modifies the behaviour of the catalyst. The effect is particularly noticeable on the trace for H₂, which is similar to that recorded on the sample

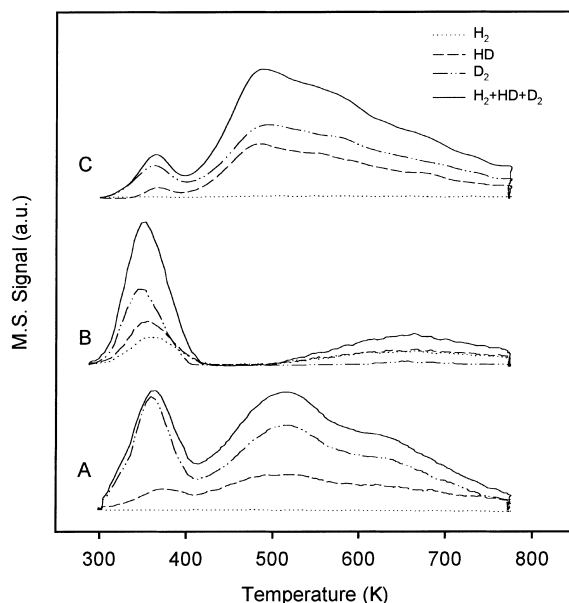


Fig. 19. TPD-MS study of the H₂, HD, and D₂ desorption from Pt(7%)/CeO₂-MS catalysts reduced at: (A) 473; (B) 773 K.; (C) The catalyst reduced at 773 K was reoxidised with flowing O₂ at 298 K (1 h), and then treated with H₂(5%)/Ar at 298 K. All these samples were further evacuated at 773 K (1 h) in a flow of Ar, then treated with flowing H₂(5%)/Ar (15 min) at 298 K, exchanged with D₂(5%)/N₂ (15 min) at 298 K. Always under flowing D₂(5%)/N₂, they were cooled to 191 K, and finally the TPD-MS experiments were run in two steps: 191–298 K (free heating); and 298–773 K (10 K min⁻¹). The reported diagrams correspond to the second step of the TPD experiments. The overall desorption traces (H₂+HD+D₂) are also depicted. Signals for HD and D₂ were corrected by taking into account its relative sensitivity with respect to H₂.

reduced at 473 K (Fig. 17(A)). As shown in Fig. 17(B), the transient desorption of H₂ was almost completely suppressed upon reduction at 773 K. The reoxidation treatment also recovers very significantly the amount of H₂/D₂ exchanged during the transient period, Table 4.

The experiment in Fig. 17(C), was completed with a TPD-MS run. The diagrams recorded for H₂, HD and D₂, and the quantitative data resulting from their integration are reported, respectively, in Fig. 19(C), and in Table 5. As in the case of the transient experiment commented on above, Fig. 17(C), the TPD-MS data deduced from Fig. 19(C), and Table 5, clearly suggest that, upon reoxidation, the behaviour of the catalyst becomes closer to that of the sample reduced

Table 5
Influence of the reduction temperature (473 or 773 K) on the chemical properties of the Pt(7%)/CeO₂-MS catalyst

Treatment	H/Pt equivalent			
	H ₂	HD	D ₂	Total
Redn 473 K/evac. 773 K/ITK 298 K/cooling D ₂ 191 K/TPD-MS 191–298 K	0.00	0.03	0.12	0.15
Redn 773 K/evac. 773 K/ITK 298 K/cooling D ₂ 191 K/TPD-MS 191–298 K	0.01	0.01	0.06	0.08
Redn 773 K/evac. 773 K/reoxn 298 K/ITK 298 K/cooling D ₂ 191 K/TPD-MS 191–298 K	0.00	0.02	0.15	0.17
Redn 473 K/evac. 773 K/ITK 298 K/cooling D ₂ 191 K/TPD-MS 298–773 K	0.00	0.14	0.33	0.47
Redn 773 K/evac. 773 K/ITK 298 K/cooling D ₂ 191 K/TPD-MS 298–773 K	0.07	0.06	0.07	0.20
Redn 773 K/evac. 773 K/reoxn 298 K/ITK 298 K/cooling D ₂ 191 K/TPD-MS 298–773 K	0.00	0.13	0.22	0.35

Quantitative estimate of the H₂, HD and D₂ desorbed during the TPD-MS experiments following the H₂/D₂ exchange studies. Data corresponding to the catalyst reduced at 773 K, further reoxidised at 298 K, and finally reduced at 298 K are also reported.

at 473 K, thus indicating a partial recovery of its chemical activity.

Since the applied reoxidation procedure should essentially modify the ceria redox state without changing the nanostructure of the platinum microcrystals, our observations strongly suggest the existence of a close relationship between metal deactivation and ceria redox state. A number of magnetic balance studies on different NM/CeO₂ catalysts give further support to this suggestion [61,92,94,101,115]. In effect, they clearly show that, upon reduction at 773 K, the degree of irreversible reduction reached by ceria, is significantly larger than that determined at 623 K or, obviously, lower temperatures.

The interpretation proposed above is also in good agreement with a recent ultraviolet photoelectron spectroscopy (UPS) study carried out on a model catalyst consisting of Rh deposited onto a CeO₂ (1 1 1)-oriented thin film [83]. As deduced from the UPS spectra recorded for rhodium, a remarkable change in the surface band bending is observed on increasing the reduction temperature up to 773 K. Associated with this electronic perturbation, drastic changes in the occupation of the electronic states near the Fermi level, with inherent loss of the hydrogen adsorption capability of the metal, are suggested to occur. These electronic phenomena are correlated with the presence of oxygen vacancies in the ceria support [83].

To summarise, it has been shown that the Pt(7%)/CeO₂-MS catalyst investigated here becomes partly deactivated upon increasing the reduction temperature from 473 to 773 K. This effect may specifically be interpreted in terms of chemical changes that occurred in the metal phase. Metal encapsulation, changes in

the metal dispersion, decoration or alloying phenomena may be discarded as the likely origin of the deactivation phenomena. All these observations, like the UPS data reported in [83], are consistent with the electronic origin of the perturbations occurring in the chemical properties of the catalyst reduced at 773 K. Likewise, the outstanding reversion of the effect by a simple reoxidation at 298 K strongly suggest that these electronic perturbations are associated with the reduction degree reached by the support.

5. Concluding remarks

Upon reviewing the ensemble of nanostructural and chemical data presented and discussed in this work, a general description of the metal/support interaction phenomena occurring in NM/CeO₂ noble metal catalysts may be proposed.

The HREM studies have allowed us to make a significant progress in our knowledge of the nanostructural evolution undergone by the NM/CeO₂ catalysts as the reduction temperature is increased. At present, HREM characterisation data corresponding to ceria-supported Rh, Pd and Pt catalysts reduced in a wide range of temperatures, from 473 to 1173 K, are available. From these studies some major conclusions may be outlined. For reduction temperatures up to 773 K, no significant nanostructural changes may be deduced from the HREM information published as yet. On ceria-supported Rh [7,18,79,93,107,169], Pt [6,29] and Pd [59] catalysts, however, the HREM and electron diffraction studies have clearly shown the existence of well-defined epitaxial relationships. This

preferential orientation of the noble metal crystallites grown on ceria may be interpreted as due to some kind of metal/support interaction. However, the effect has been observed with independence of the reduction temperature, i.e. on catalysts reduced well below 773 K [93]. Accordingly, the information presently available does allow to correlate changes in the chemical properties of the catalysts with the existence of a metal/support epitaxial relationship.

The HREM studies also allow us to exclude the metal decoration and alloying phenomena as relevant factors in determining the chemical behaviour of the NM/CeO₂ reduced at 773 K or lower temperatures. This conclusion, which is supported by all the experimental HREM data reported as yet, is particularly noticeable, because many authors [60,69,117,119,125,145] have speculated in the past about their role in the deactivation of catalysts reduced at $T_{\text{redn}} \leq 773$ K.

By contrast, the occurrence of decoration phenomena is now well established for $T_{\text{redn}} > 773$ K. They were first reported on Rh/CeO₂ reduced at 973 K [93], and later on Pt/CeO₂ [29,31], also reduced at 973 K, and Pd/CeO₂ reduced at 873 [63] and 973 K [59]. The existence of a crystallographically well-defined alloy phase (CePt₅) has only been unequivocally established from the HREM studies performed on a Pt/CeO₂ catalyst reduced even at a higher temperature, 1173 K [29]. As already discussed in Section 3.2.1.1 of this work, the formation of an f.c.c. solid solution of Ce in Pd with a lattice parameter slightly larger (2.1–2.3%) than that of the metal has been reported to occur on Pd/CeO₂ catalysts reduced at 873–973 K [59,63]. Though reduction temperatures as high as 1180 K were applied, stoichiometrically well-defined Pd–Ce intermetallic compounds could not be observed [59]. For Rh/CeO₂, no evidence of alloying has been reported as yet, even on catalysts reduced at 1173 K [93].

HREM studies have also provided interesting pieces of information about the nanostructural effects induced by the reoxidation treatments. Reoxidation temperatures ranging from 373 to 1173 K have been investigated. Likewise, they have been applied to samples pre-reduced at temperatures up to 1173 K. In accordance with these studies, on catalysts reduced at $T_{\text{redn}} \leq 773$ K, the reoxidation treatments up to 773 K lead to minor nanostructural changes in the catalysts. Also, interesting is that, in contrast with that

reported for NM/TiO₂ catalysts [5,6,8], the reoxidation at 773 K, does not allow the NM/CeO₂ catalysts to recover from the decoration or alloying phenomena. Much higher reoxidation temperatures are needed to achieve this objective.

Regarding the chemical evolution undergone by the NM/CeO₂ catalysts on increasing the reduction temperature, on the basis of chemisorption, mainly dealing with H₂ [7,16,30,49,80,81,83,95,101,107,117,150] and CO [19,26,35,125], and catalytic activity [16,22,43,63,119,125,151] data, many authors have suggested the occurrence of significant deactivation effects at $T_{\text{redn}} \leq 773$ K. In particular, the hydrogenolysis of alkanes seems to be very sensitive to the reduction conditions [16,22,43,119,151]. In the case of the chemisorption studies, though examples of both strong [69,83,117,125] and minor [62] perturbation effects may be found in the literature, significant but partial deactivation is the most commonly observed phenomenon for reduction temperatures up to 773 K. This is also the case of the Pt(7%)/CeO₂-SM catalyst investigated in this work. The results reported on this latter sample are particularly interesting because of its very specific nanostructural characteristics. In effect, as already noted, this sample was on-purpose prepared in such way as to allow that some of the major side effects disturbing the interpretation of the chemical results were avoided. Likewise, the experimental approach followed in the hydrogen chemisorption studies, particularly the low-temperature TPD-MS data, and the H₂/D₂ exchange experiments have also helped very much in establishing the occurrence of chemical deactivation effects specifically associated with the supported metal phase. For this catalyst, within the range of moderate reduction temperatures, $T_{\text{redn}} \leq 773$ K, metal encapsulation, decoration or alloying phenomena may be excluded as relevant factors in determining the observed chemical changes. Accordingly, electronic perturbations that occurred in the supported metal phase should be considered as the key factor. Also worth outlining is that the recovery effect induced by a reoxidation treatment at 298 K should be interpreted as a proof of the relationship existing between chemical deactivation, electronic state of the platinum crystallites and ceria reduction degree.

Assuming the above interpretation, the intensity of the deactivation effects that occurred in NM/CeO₂

catalysts reduced at temperatures not higher than 773 K may be sensitive to a number of variables. Even if strongly disturbing factors like the presence of chlorine are excluded, the nature of the metal, its actual dispersion, or the microstructure of the ceria sample used as support may reasonably have a significant influence. In this respect, it would be noted that some very recent studies on both, ceria, and NM/CeO₂ samples have shown that their catalytic and specifically, their redox properties, are significantly influenced by the microstructural characteristics of the oxide samples [85,194–196]. In accordance with this, it would not be unexpected that different authors had reported deactivation effects of variable intensity. Nevertheless, it should be stressed that, in contrast with that often reported for NM/TiO₂ [3,7,16], on NM/CeO₂ catalysts reduced at temperatures not higher than 773 K complete inhibition of their hydrogen chemisorption capability is seldom observed. Moreover, the very few available data for the hydrogen adsorption on NM/CeO₂ catalysts reduced at 973 K [81,93,150], i.e. under conditions leading to the onset of the metal decoration effects, show that, even at such a high temperature, no suppression of the chemisorption capability occurs.

To summarise, the results on NM/CeO₂ catalysts reviewed in this work suggest that, from a phenomenological point of view, the evolution undergone by the chemical and nanostructural properties of these systems is parallel to the one characterising the SMSI effect in NM/TiO₂ catalysts. For Rh/TiO₂ [9–11], as the reduction temperature is increased, electronic perturbations of the supported metal phase would be observed first, the onset of the decoration phenomena occurring as a second step, at higher reduction temperatures. On NM/CeO₂ catalysts, a rather similar description would account for the experimental observations discussed here. However, some relevant differences should be noted between NM/CeO₂ and NM/TiO₂ catalysts. In the former case, the reduction conditions leading to the appearance of the decoration effects is significantly shifted towards higher temperatures. Likewise, the behaviour against reoxidation of the decorated samples is also different. For NM/TiO₂ catalysts, 773 K is a high enough reoxidation temperature as to recover them from the decorated state. By contrast, the HREM studies presented here have clearly shown that such a reoxidation temperature

does not guarantee an effective segregation of the metal and overlayers of ceria phases. In fact, the recovery of the NM/CeO₂ catalyst by reoxidation at or below 773 K should actually be interpreted as an indication of a previous reduction treatment not hard enough as to induce the decoration or alloying phenomena; i.e. the electronic effects would probably be mainly responsible for the observed deactivation.

Acknowledgements

This work has been supported by the CICYT (Project: MAT96-0931), the DIGCYT (Project: PB95-1257), the Junta de Andalucía, and the TMR Program of the EU (CEZIRENCAT Project, Contract: FMRX-CT96-0060). We also thank Johnson Matthey for a loan of noble metals. The HREM images reported in this work were obtained at the Electron Microscopy facilities of the University of Cádiz.

References

- [1] S.J. Tauster, S.C. Fung, R.L. Garten, *J. Am. Chem. Soc.* 100 (1978) 170.
- [2] S.J. Tauster, *Acc. Chem. Res.* 20(11) (1987) 389.
- [3] G.L. Haller, D.E. Resasco, *Adv. Catal.* 36 (1989) 173.
- [4] A.D. Logan, E.J. Braunschweig, A.K. Datye, D.J. Smith, *Langmuir* 4 (1988) 827.
- [5] E.J. Braunschweig, A.D. Logan, A.K. Datye, D.J. Smith, *J. Catal.* 118 (1989) 227.
- [6] A.K. Datye, D. Kalakkad, M.H. Yao, D.J. Smith, *J. Catal.* 155 (1995) 148.
- [7] S. Bernal, J.J. Calvino, M.A. Cauqui, G.A. Cifredo, A. Jobacho, J.M. Rodríguez-Izquierdo, *Appl. Catal.* 99 (1993) 1.
- [8] S. Bernal, F.J. Botana, J.J. Calvino, C. López, J.A. Pérez Omil, J.M. Rodríguez-Izquierdo, *J. Chem. Soc., Faraday Trans.* 92 (1996) 2799.
- [9] J.P. Belzunegui, J. Sanz, J.M. Rojo, *J. Am. Chem. Soc.* 112 (1990) 4066.
- [10] J.P. Belzunegui, J.M. Rojo, J. Sanz, *J. Phys. Chem.* 95 (1991) 3464.
- [11] J. Sanz, J.P. Belzunegui, J.M. Rojo, *J. Am. Chem. Soc.* 114 (1992) 6749.
- [12] K. Otsuka, M. Hatano, A. Morikawa, *J. Catal.* 79 (1983) 493.
- [13] A. Laachir, V. Perrichon, A. Badri, J. Lamotte, E. Catherine, J.C. Lavalley, J. El Fallah, L. Hilaire, F. Le Normand, E. Quéméré, *J. Chem. Soc., Faraday Trans.* 87 (1991) 1601.

- [14] V. Perrichon, A. Laachir, G. Bergeret, R. Frety, L. Tournayan, O. Touret, *J. Chem. Soc., Faraday Trans.* 90(5) (1994) 773.
- [15] S. Bernal, J.J. Calvino, G.A. Cifredo, J.M. Gatica, J.A. Pérez Omil, J. Pintado, *J. Chem. Soc., Faraday Trans.* 89 (1993) 3499.
- [16] P. Meriaudeau, J.F. Dutel, M. Dufaux, C. Naccache, *Stud. Surf. Sci. Catal.* 11 (1982) 95.
- [17] P. Meriaudeau, J.F. Dutel, M. Dufaux, C. Naccache, Strong metal support interactions, *ACS Symp. Ser.* 298 (1986) 118.
- [18] M. Pan, J.M. Cowley, R. García, *Micron. Microscop. Acta* 18 (1987) 165.
- [19] S. Bernal, F.J. Botana, J.J. Calvino, G.A. Cifredo, R. García, J.M. Rodríguez-Izquierdo, *Catal. Today* 2 (1988) 653.
- [20] Y. Zhou, M. Nakashima, J.M. White, *J. Phys. Chem.* 92 (1988) 812.
- [21] D.W. Daniel, *J. Phys. Chem.* 92 (1988) 3891.
- [22] A. Maubert, G.A. Martin, H. Praliaud, P. Turlier, *React. Kinet. Catal. Lett.* 24 (1984) 183.
- [23] C. Sudhakar, M.A. Vannice, *Appl. Catal.* 14 (1985) 47.
- [24] I. Akalay, M.F. Guilleux, J.F. Tempere, D. Delafosse, *J. Chem. Soc., Faraday Trans.* 1(83) (1987) 1137.
- [25] M.G. Sanchez, J.L. Gazquez, *J. Catal.* 104 (1987) 120.
- [26] A. Trovarelli, *Catal. Rev.-Sci. Eng.* 38(4) (1996) 439.
- [27] B. Harrison, A.F. Diwell, C. Hallett, *Platinum Metals Rev.* 32(2) (1988) 73.
- [28] T. Bunluesin, R.J. Gorte, G.W. Graham, *Appl. Catal. B* 15 (1998) 107.
- [29] S. Bernal, J.J. Calvino, J.M. Gatica, C. Larese, C. López Cartes, J.A. Pérez Omil, *J. Catal.* 169 (1997) 510.
- [30] C. Leitenburg, A. Trovarelli, J. Kaspar, *J. Catal.* 166 (1997) 98.
- [31] S. Bernal, M.A. Cauqui, G.A. Cifredo, J.M. Gatica, C. Larese, J.A. Pérez Omil, *Catal. Today* 29 (1996) 77.
- [32] S. Bernal, J.M. Gatica, C. Larese, J.A. Pérez Omil, J.M. Rodríguez-Izquierdo, E. Herrero, O. Anunziata, C. Pérez (Eds.), *XV Simposio Iberoamericano de Catálisis*, Unica Edición, Córdoba, Argentina, 1996, p. 7.
- [33] T. Bunluesin, E.S. Putna, R.J. Gorte, *Catal. Lett.* 41 (1996) 1.
- [34] C. Hardacre, T. Rayment, R.M. Lambert, *J. Catal.* 158 (1996) 102.
- [35] S.E. Golunski, H.A. Hatcher, R.R. Rajaram, T.J. Truex, *Appl. Catal. B* 5 (1995) 367.
- [36] C. Hardacre, G.M. Roe, R.M. Lambert, *Surf. Sci.* 326 (1995) 1.
- [37] C. Hardacre, R.M. Ormerod, R.M. Lambert, *J. Phys. Chem.* 98 (1994) 10901.
- [38] J.P. Holgado, G. Munuera, *Stud. Surf. Sci. Catal.* 96 (1995) 109.
- [39] D.S. Kalakkad, A.K. Datye, H.J. Robota, *J. Catal.* 148 (1994) 729.
- [40] W. Liu, A.F. Sarofim, M. Flytzani-Stephanopoulos, *Appl. Catal. B* 4 (1994) 167.
- [41] T.X.T. Sayle, S.C. Parker, C.R.A. Catlow, *J. Phys. Chem.* 98 (1994) 13625.
- [42] T. Yamada, K. Kayano, M. Funabiki, *Stud. Surf. Sci. Catal.* 77 (1993) 329.
- [43] D. Kalakkad, A.K. Datye, H. Robota, *Appl. Catal. B* 1 (1992) 191.
- [44] J.G. Nunan, M.J. Cohn, J.T. Donner, *Catal. Today* 14 (1992) 277.
- [45] G.S. Zafiris, R.J. Gorte, *Surf. Sci.* 276 (1992) 86.
- [46] T. Chojnacki, K. Krause, L.D. Schmidt, *J. Catal.* 128 (1991) 161.
- [47] A. Dauscher, G. Maire, *J. Molec. Catal.* 69 (1991) 259.
- [48] J. El Fallah, F. Le Normand, S. Boujana, A. Kiennemann, *Eur. J. Solid State Inorg. Chem.* 28 (1991) 433.
- [49] P.J. Levy, M. Primet, *Appl. Catal.* 70 (1991) 263.
- [50] P. Lööf, B. Kasemo, S. Andersson, A. Frestad, *J. Catal.* 130 (1991) 181.
- [51] L.L. Murrell, S.J. Tauster, D.R. Anderson, *Stud. Surf. Sci. Catal.* 71 (1991) 275.
- [52] H.D. Cochrane, J.L. Hutchinson, D. White, G.M. Parkinson, C. Dupas, A.J. Scott, *Ultramicroscopy* 34 (1990) 10.
- [53] A. Dauscher, L. Hilaire, L. Le Normand, W. Müller, G. Maire, A. Vasquez, *Surf. Interf. Anal.* 16 (1990) 341.
- [54] M. Primet, M. El Azhar, R. Frety, M. Guenin, *Appl. Catal.* 59 (1990) 153.
- [55] M.F. Luo, Z.Y. Hou, X.X. Yuan, X.M. Zheng, *Catal. Lett.* 50 (1998) 205.
- [56] L. Filotti, A. Bensalem, F. Bozon-Verduraz, G.A. Shafeev, V.V. Voronov, *Appl. Surf. Sci.* 109 (1997) 249.
- [57] T. Bunluesin, R.J. Gorte, G.W. Graham, *Appl. Catal. B* 14 (1997) 105.
- [58] R. Craciun, B. Shereck, R.J. Gorte, *Catal. Lett.* 51 (1998) 149.
- [59] L. Kepinski, M. Wolcyrz, *Appl. Catal. A* 150 (1997) 197.
- [60] A. Bensalem, J.C. Muller, D. Tessier, F. Bozon-Verduraz, *J. Chem. Soc., Faraday Trans.* 92(17) (1996) 3233.
- [61] A. Bensalem, F. Bozon-Verduraz, V. Perrichon, *J. Chem. Soc., Faraday Trans.* 91 (1995) 2185.
- [62] H. Cordatos, R.J. Gorte, *J. Catal.* 159 (1996) 112.
- [63] L. Kepinski, M. Wolcyrz, J. Okal, *J. Chem. Soc., Faraday Trans.* 91(3) (1995) 507.
- [64] R. Souza Monteiro, F. Bellot Noronha, L. Chaloub Dieguez, M. Schmal, *Appl. Catal. A* 131 (1995) 89.
- [65] L. Fan, K. Fujimoto, *J. Catal.* 150 (1994) 217.
- [66] A. Badri, C. Binet, J.C. Lavalley, *J. Phys. Chem.* 100 (1996) 8363.
- [67] C. Binet, A. Badri, M. Boutonnet-Kizling, J.C. Lavalley, *J. Chem. Soc., Faraday Trans.* 90 (1994) 1023.
- [68] A. Bensalem, G. Shafeev, F. Bozon-Verduraz, *Catal. Lett.* 18 (1993) 165.
- [69] C. Binet, A. Jadi, J.C. Lavalley, M. Boutonnet-Kizling, *J. Chem. Soc., Faraday Trans.* 88 (1992) 2079.
- [70] M. Wolcyrz, L. Kepinski, *J. Solid State Chem.* 99 (1992) 409.
- [71] A. Trovarelli, G. Dolcetti, C. Leitenburg, J. Kaspar, *Stud. Surf. Sci. Catal.* 75 (1993) 2781.
- [72] J.L. Duplan, H. Praliaud, *Appl. Catal.* 67 (1991) 325.
- [73] F. Le Normand, J. Barrault, R. Breault, L. Hilaire, A. Kiennemann, *J. Phys. Chem.* 95 (1991) 257.

- [74] Z. Shyu, K. Otto, L.H. Watkins, G.W. Graham, R.K. Belitz, H.S. Gandhi, *J. Catal.* 114 (1988) 23.
- [75] C. Sudhakar, M.A. Vannice, *J. Catal.* 95 (1985) 227.
- [76] M.D. Mitchell, M.A. Vannice, *Ind. Eng. Chem. Fundam.* 23 (1984) 88.
- [77] S. Imamura, T. Yamashita, R. Hamada, Y. Saito, Y. Nakao, N. Tsuda, C. Kaito, *J. Molec. Catal. A* 129 (1998) 249.
- [78] S. Bernal, J.J. Calvino, M.A. Cauqui, J.A. Pérez Omil, J. Pintado, J.M. Rodríguez-Izquierdo, *Appl. Catal. B* 16 (1998) 127.
- [79] S. Bernal, F.J. Botana, J.J. Calvino, C. López Cartes, J.A. Pérez Omil, J.M. Rodríguez-Izquierdo, *Ultramicroscopy* 72 (1998) 135.
- [80] D.I. Kondarides, X.E. Verykios, *J. Catal.* 174 (1998) 52.
- [81] P. Fornasiero, J. Kaspar, M. Graziani, *J. Catal.* 167 (1997) 576.
- [82] S. Bernal, G. Blanco, M.A. Cauqui, M.P. Corchado, J. Pintado, J.M. Rodríguez-Izquierdo, *Chem. Commun.* (1997) 1545.
- [83] A. Pfau, J. Sanz, K.D. Schierbaum, W. Göpel, J.P. Belzungeui, J.M. Rojo, *Stud. Surf. Sci. Catal.* 101 (1996) 931.
- [84] A. Martínez Arias, J. Soria, J.C. Conesa, *J. Catal.* 168 (1997) 364.
- [85] E.S. Putna, J.M. Vohs, R.J. Gorte, *Catal. Lett.* 45 (1997) 143.
- [86] J. Stubenrauch, J.M. Vohs, *Catal. Lett.* 47 (1997) 21.
- [87] J. Cunningham, J.N. Hickey, R. Cataluna, J.C. Conesa, J. Soria, A. Martínez-Arias, *Stud. Surf. Sci. Catal.* 101 (1996) 681.
- [88] D. Demri, L. Chateau, J.P. Hindermann, A. Kiennemann, M.M. Bettahar, *J. Molec. Catal.* 104 (1996) 237.
- [89] E.S. Putna, J.M. Vohs, R.J. Gorte, *J. Phys. Chem.* 100 (1996) 17862.
- [90] J. Stubenrauch, J.M. Vohs, *J. Catal.* 159 (1996) 50.
- [91] R. Taha, D. Martin, S. Kacimi, D. Duprez, *Catal. Today* 29 (1996) 89.
- [92] S. Bernal, J.J. Calvino, G.A. Cifredo, J.M. Gatica, J.A. Pérez Omil, A. Laachir, V. Perrichon, *Stud. Surf. Sci. Catal.* 96 (1995) 419.
- [93] S. Bernal, F.J. Botana, J.J. Calvino, G.A. Cifredo, J.A. Pérez Omil, J. Pintado, *Catal. Today* 23 (1995) 219.
- [94] S. Bernal, J.J. Calvino, G.A. Cifredo, J.M. Rodríguez-Izquierdo, *J. Phys. Chem.* 99 (1995) 11794.
- [95] C. Leitenburg, A. Trovarelli, *J. Catal.* 156 (1995) 171.
- [96] A. Pfau, K.D. Schierbaum, W. Göpel, *Surf. Sci.* 331–333 (1995) 1479.
- [97] E.S. Putna, J. Stubenrauch, J.M. Vohs, R.J. Gorte, *Langmuir* 11 (1995) 4832.
- [98] A. Trovarelli, C. Leitenburg, G. Dolcetti, J. Llorca, *J. Catal.* 151 (1995) 111.
- [99] T. Bunluesin, H. Cordatos, R.J. Gorte, *J. Catal.* 157 (1995) 222.
- [100] S. Bernal, G. Blanco, J.J. Calvino, G.A. Cifredo, J.A. Pérez Omil, J.M. Pintado, A. Varo, *Stud. Surf. Sci. Catal.* 82 (1994) 507.
- [101] S. Bernal, J.J. Calvino, G.A. Cifredo, A. Laachir, V. Perrichon, J.M. Herrmann, *Langmuir* 10 (1994) 717.
- [102] J. Cunningham, D. Cullinane, F. Farrell, M.A. Morris, A.K. Datye, D. Kalakkad, *Stud. Surf. Sci. Catal.* 96 (1995) 237.
- [103] J. El Fallah, S. Boujana, H. Dexpert, A. Kiennemann, J. Majerus, O. Touret, F. Villain, F. Le Normand, *J. Phys. Chem.* 98 (1994) 5522.
- [104] A. Laachir, V. Perrichon, S. Bernal, J.J. Calvino, G.A. Cifredo, *J. Molec. Catal.* 89 (1994) 391.
- [105] C. Padeste, N.W. Cant, D.L. Trimm, *Catal. Lett.* 28 (1994) 301.
- [106] C. Padeste, N.W. Cant, D.L. Trimm, *Catal. Lett.* 24 (1994) 95.
- [107] S. Bernal, F.J. Botana, J.J. Calvino, M.A. Cauqui, G.A. Cifredo, A. Jobacho, J. Pintado, J.M. Rodríguez-Izquierdo, *J. Phys. Chem.* 97 (1993) 4118.
- [108] S. Bernal, F.J. Botana, J.J. Calvino, G.A. Cifredo, J.A. Pérez Omil, *Inst. Phys. Conf. Ser.* 138(Section)10 (1993) 485.
- [109] T. Shido, Y. Iwasawa, *J. Catal.* 141 (1993) 71.
- [110] J. Soria, A. Martínez-Arias, J.M. Coronado, J.C. Conesa, *Appl. Surf. Sci.* 70/71 (1993) 245.
- [111] J.P. Warren, X. Zhang, J.E.T. Andersen, R.M. Lambert, *Surf. Sci.* 287/288 (1993) 222.
- [112] G.S. Zafiris, R.J. Gorte, *J. Catal.* 139 (1993) 561.
- [113] G.S. Zafiris, R.J. Gorte, *J. Catal.* 143 (1993) 86.
- [114] J. Barbier Jr., F. Marsollier, D. Duprez, *Appl. Catal. A* 90 (1992) 11.
- [115] S. Bernal, J.J. Calvino, G.A. Cifredo, J.M. Rodríguez-Izquierdo, V. Perrichon, A. Laachir, *J. Chem. Soc. Chem. Comm.* (1992) 460.
- [116] S. Bernal, J.J. Calvino, G.A. Cifredo, J.M. Rodríguez-Izquierdo, V. Perrichon, A. Laachir, *J. Catal.* 137 (1992) 1.
- [117] J. Cunningham, D. Cullinane, J. Sanz, J.M. Rojo, J. Soria, J.L.G. Fierro, *J. Chem. Soc., Faraday Trans.* 88(21) (1992) 3233.
- [118] J. Soria, A. Martínez-Arias, J.C. Conesa, *Vacuum* 43 (1992) 437.
- [119] A. Trovarelli, G. Dolcetti, C. Leitenburg, J. Kaspar, P. Finetti, A. Santoni, *J. Chem. Soc., Faraday Trans.* 88 (1992) 1311.
- [120] S. Bernal, J.J. Calvino, G.A. Cifredo, A. Jobacho, J.M. Rodríguez-Izquierdo, *J. Rare Earths (Special Issue)* 2 (1991) 838.
- [121] A.R. González-Elipse, J.P. Holgado, R. Alvarez, J.P. Espinós, A. Fernández, G. Munuera, in: H.H. Brongersma, R.A. van Santen (Eds.), *Fundamental Aspects of Heterogeneous Catalysis Studied by Particle Beams*, New York, 1991, p. 227.
- [122] G. Munuera, A. Fernández, A.R. González-Elipse, *Stud. Surf. Sci. Catal.* 71 (1991) 207.
- [123] A. Trovarelli, C. Leitenburg, G. Dolcetti, *J. Chem. Soc. Chem. Comm.* (1991) 472.
- [124] S. Bernal, F.J. Botana, J.J. Calvino, G.A. Cifredo, R. García, J.M. Rodríguez-Izquierdo, *Ultramicroscopy* 34 (1990) 60.
- [125] J. Cunningham, S. O'Brien, J. Sanz, J.M. Rojo, J. Soria, J.L.G. Fierro, *J. Molec. Catal.* 57 (1990) 379.

- [126] J.C. Lavalley, J. Saussey, J. Lamotte, R. Breault, J.P. Hindermann, A. Kiennemann, *J. Phys. Chem.* 94 (1990) 5941.
- [127] Y. Niwa, K. Aika, *J. Catal.* 162 (1996) 138.
- [128] M.J. Saeki, H. Uchida, M. Watanabe, *Catal. Lett.* 26 (1994) 149.
- [129] L.A. Bruce, M. Hoang, A.E. Hughes, T.W. Turney, *Appl. Catal. A* 100 (1993) 51.
- [130] L. Tournayan, N.R. Marcilio, R. Frety, *Appl. Catal.* 78 (1991) 31.
- [131] R. Frety, P.N. Da Silva, M. Guenin, *Appl. Catal.* 58 (1990) 175.
- [132] P.N. Da Silva, M. Guenin, C. Lecrercq, R. Frety, *Appl. Catal.* 54 (1989) 203.
- [133] W. Liu, M. Flytzani-Stephanopoulos, *J. Catal.* 153 (1995) 304.
- [134] W. Liu, M. Flytzani-Stephanopoulos, *J. Catal.* 153 (1995) 317.
- [135] E.A. Shaw, A.P. Walker, T. Rayment, R.M. Lambert, *J. Catal.* 134 (1992) 747.
- [136] S. Tang, J. Lin, K.L. Tan, *Catal. Lett.* 51 (1998) 169.
- [137] V.D. Belyaev, T.I. Politova, O.A. Mar'ina, V.A. Sobyenin, *Appl. Catal. A* 133 (1995) 47.
- [138] C. Colliex, E. Lefèvre, M. Tencé, *Inst. Phys. Conf. Ser.* 138 (1993) 25.
- [139] S. Kacimi, J. Barbier Jr., R. Taha, D. Duprez, *Catal. Lett.* 22 (1993) 343.
- [140] G. Wrobel, M.P. Sohler, A. D'Huyse, J.P. Bonnelle, J.P. Marcq, *Appl. Catal. A* 101 (1993) 73.
- [141] T. Inui, *J. Alloys Comp.* 193 (1993) 47.
- [142] E. Ramarosan, J.F. Tempere, M.F. Guilleux, F. Vergand, H. Roulet, G. Dufour, *J. Chem. Soc., Faraday Trans.* 88 (1992) 1211.
- [143] M.P. Sohler, G. Wrobel, J.P. Bonnelle, J.P. Marcq, *Appl. Catal. A* 84 (1992) 169.
- [144] J. Barrault, A. Alouche, *Appl. Catal.* 58 (1990) 255.
- [145] J. Barrault, A. Alouche, V. Paul-Boncour, L. Hilaire, A. Percheron-Guegan, *Appl. Catal.* 46 (1989) 269.
- [146] J. Barrault, A. Alouche, *Appl. Catal.* 46 (1989) 269.
- [147] Z.L. Wang, C. Colliex, V. Paul-Boncour, A. Percheron-Guegan, J.C. Achard, J. Barrault, *J. Catal.* 105 (1987) 120.
- [148] M.F. Luo, Y.J. Zhong, X.X. Yuan, X.M. Zheng, *Appl. Catal. A* 162 (1997) 121.
- [149] A. Aboukaïs, A. Bannani, C. Damonier-Dulongpont, E. Abiad, G. Wrobel, *Colloids Surfaces A* 115 (1996) 171.
- [150] S. Bernal, M.A. Cauqui, G.A. Cifredo, J.M. Gatica, C. Larese, J.A. Pérez Omil, *Catal. Today* 29 (1996) 77.
- [151] P. Turlier, H. Praliaud, P. Moral, G.A. Martin, J.A. Dalmon, *Appl. Catal.* 19 (1985) 287.
- [152] J.M. Herrmann, E. Ramarosan, J.F. Tempere, M.F. Guilleux, *Appl. Catal.* 53 (1989) 117.
- [153] M. Pijolat, M. Prin, M. Soustelle, O. Touret, P. Nortier, *J. Chem. Soc., Faraday Trans.* 91 (1995) 3941.
- [154] V. Perrichon, A. Laachir, S. Abouarnadasse, O. Touret, G. Blanchard, *Appl. Catal. A* 129 (1995) 69.
- [155] J.R. Katzer, A.W. Sleight, P. Gajardo, J.B. Michel, E.F. Gleason, S. McMillan, *Disc. Faraday Soc.* 72 (1981) 121.
- [156] J.L.G. Fierro, J. Soria, J. Sanz, J.M. Rojo, *J. Solid State Chem.* 66 (1987) 154.
- [157] S. Bernal, J.J. Calvino, G.A. Cifredo, J.M. Gatica, J.A. Pérez Omil, J.M. Pintado, *J. Chem. Soc., Faraday Trans.* 89 (1993) 3499.
- [158] F. Le Normand, L. Hilaire, K. Kili, G. Krill, G. Maire, *J. Phys. Chem.* 92 (1988) 2561.
- [159] C. Li, Y. Sakata, T. Arai, K. Domen, K. Maruya, T. Onishi, *J. Chem. Soc., Faraday Trans.* 85 (1989) 929.
- [160] C. Li, Y. Sakata, T. Arai, K. Domen, K. Maruya, T. Onishi, *J. Chem. Soc., Faraday Trans.* 85 (1989) 1451.
- [161] F. Bozon-Verduraz, A. Bensalem, *J. Chem. Soc., Faraday Trans.* 90 (1994) 653.
- [162] C. Li, Y. Sakata, T. Arai, K. Domen, K. Maruya, T. Onishi, *J. Chem. Soc. Chem. Comm.* (1991) 410.
- [163] M. Pan, R. García, D.J. Smith, J.M. Cowley, G.A. Cifredo, *Proceedings of the 47th Annual Meeting Electron Microscopy Society of America*, 1989, p. 256.
- [164] A.A. Kaïs, A. Bennami, C.F. Aissi, G. Wrobel, M. Guelton, *J. Chem. Soc., Faraday Trans.* 88 (1992) 1321.
- [165] T. Jin, Y. Zhou, G.J. Mains, J.M. White, *J. Phys. Chem.* 91 (1987) 5931.
- [166] C. Binet, A. Badri, J.C. Lavalley, *J. Phys. Chem.* 98 (1994) 6392.
- [167] C. Binet, A. Jadi, J.C. Lavalley, *J. Chim. Phys.* 88 (1991) 499.
- [168] A. Badri, J. Lamotte, J.C. Lavalley, A. Laachir, V. Perrichon, O. Touret, G.N. Sauvion, E. Quéméré, *Eur. J. Solid State Inorg. Chem.* 28 (1991) 445.
- [169] M. Pan, Ph.D. Thesis, Arizona State University, 1991.
- [170] S. Bernal, F.J. Botana, R. García, Z. Kang, M.L. López, M. Pan, F. Ramírez, J.M. Rodríguez-Izquierdo, *Catal. Today* 2 (1988) 653.
- [171] R.V. Hardeveld, F. Hartog, *Surf. Sci.* 15 (1969) 189.
- [172] V. Radmilovic, M.A. O'Keefe, *Proceedings of the 53rd MSA*, vol. 53, 1995, p. 564.
- [173] B.J. Cooper, *Platinum Metals Rev.* 38 (1994) 2.
- [174] W. Bronger, *J. Less-Common Met.* 12 (1967) 63.
- [175] J. Le Roy, J.M. Moreau, D. Paccard, *Acta Cryst. B* 34 (1978) 9.
- [176] V.B. Compton, B.T. Matthias, *Acta Cryst.* 12 (1959) 651.
- [177] A.E. Dwight, R.A. Conner, J.W. Downey, *Acta Cryst.* 18 (1965) 837.
- [178] J. Summers, S.A. Ausen, *J. Catal.* 58 (1979) 131.
- [179] C. Serre, F. Garin, G. Belot, G. Maire, *J. Catal.* 141 (1993) 1.
- [180] T. Jin, T. Okuhara, G.J. Mains, J.M. White, *J. Phys. Chem.* 91 (1987) 3310.
- [181] D.D. Beck, T.W. Capehart, C. Wong, D.N. Belton, *J. Catal.* 144 (1993) 311.
- [182] A.D. Logan, K. Sharoudi, A.K. Datye, *J. Phys. Chem.* 95 (1991) 5568.
- [183] A. Wold, R.J. Arnott, W.J. Croft, *Inorg. Chem.* 2 (1963) 972.
- [184] L.A. Carol, G.S. Mann, *Oxidat. Metals.* 34 (1990) 1.
- [185] S.E. Wanke, P.C. Flynn, *Catal. Rev.-Sci. Eng.* 12 (1975) 93.

- [186] G.C. Bond, *Stud. Surf. Sci. Catal.* 17 (1983) 1.
- [187] J.P. Belzunegui, J.M. Rojo, J. Sanz, *J. Chem. Soc., Faraday Trans.* 85 (1989) 4287.
- [188] S. Bernal, M. García Basallote, J.M. Gatica, M. Pozo, unpublished results (1998).
- [189] G.C. Bond, P.B. Wells, *Appl. Catal.* 18 (1985) 221.
- [190] G.C. Bond, P.B. Wells, *Appl. Catal.* 18 (1985) 225.
- [191] J.W. Geus, P.B. Wells, *Appl. Catal.* 18 (1985) 231.
- [192] A. Frennet, P.B. Wells, *Appl. Catal.* 18 (1985) 243.
- [193] P.B. Wells, *Appl. Catal.* 18 (1985) 259.
- [194] H. Cordatos, T. Bunluesin, J. Stubenrauch, J.M. Vohs, R.J. Gorte, *J. Phys. Chem.* 100 (1996) 785.
- [195] E.S. Putna, J.M. Vohs, R.J. Gorte, *J. Phys. Chem.* 100 (1996) 17862.
- [196] H. Cordatos, D. Ford, R.J. Gorte, *J. Phys. Chem.* 100 (1996) 18128.